Dye-Sensitized Heterogeneous Photocatalysts for Green Redox Reactions

Gianna Reginato,*[a] Lorenzo Zani,*[a] Massimo Calamante,[a,b] Alessandro Mordini[a,b] and Alessio Dessì[a]

[a] Dr. G. Reginato, Dr. Lorenzo Zani, Dr. M. Calamante, Dr. A. Mordini, Dr. A. Dessì, Institute of Chemistry of Organometallic Compounds (CNR-ICCOM), Via Madonna del Piano 10, 50019 Sesto Fiorentino, Italy; [b] Dr. M. Calamante, Dr. A. Mordini, Department of Chemistry "U. Schiff", University of Florence, Via della Lastruccia 13, 50019 Sesto Fiorentino, Italy.

Abstract: Conversion of sunlight into chemical energy has been the subject of intense research efforts in recent years, due to the possibility to store the enormous amount of energy continuously provided by the Sun in the form of useful "solar fuels". To allow such process, suitable photocatalysts are required, which are usually obtained by combination of different inorganic materials or by self-assembly of molecular components on semiconductor surfaces: accordingly, they are capable to carry out several different processes such as light harvesting, substrate binding, electron transport, storage and transfer. Among the photocatalytic systems developed to date, heterogeneous dye-sensitized semiconductors decorated with various electrocatalysts received particular attention, thanks to their favorable properties of tunable absorption spectrum, high stability and adaptability to different reactions. In this paper, we will review some selected examples of application of such photocatalysts to two main reactions, namely H^+ reduction to H_2 and CO_2 conversion to C_1-building blocks (CO, formate), which are among the most important transformations in the field of so-called "artificial photosynthesis".

1. Introduction

The constant increase in global energy consumption,[1] coupled with rising environmental concerns, demands for a urgent transition in energy production from fossil fuels to renewable resources.[2] In this context, harvesting of solar radiation appears particularly promising, since sunlight is abundant, widely distributed on Earth's surface, virtually inexhaustible and free. Accordingly, along several decades, massive efforts have been dedicated to the discovery of new materials for the efficient conversion of solar light into electric current by means of different kinds of photovoltaic (PV) devices.[3–7] Despite the great successes achieved in this field, it's worth noting that currently electricity demand does not represent the largest portion of global energy needs, which is instead constituted by fuels, mostly used for transportation and heating.[8] Furthermore, solar radiation is inherently intermittent and its intensity and duration are affected by several different factors (geographical location, seasonal variability, weather). For all these reasons, an alternative approach has been proposed, namely to convert solar radiation directly into storable, energy rich compounds (the so-called "solar fuels"), starting from abundant and low energy raw materials such as water.[9] Such compounds could thus represent a reliable source of renewable fuels for a variety of

applications (*e. g.* electricity generation in fuel cells), contributing to enhance the sustainability and security of global energy supply.[10]

The photocatalytic conversion of sunlight and suitable starting materials into solar fuels is often called "artificial photosynthesis",[11] that is H_2 production from water photosplitting and production of a variety of carbon-based species (such as methane, methanol, CO, formate etc.) from CO_2 reduction.[12,13] These are often complex, sequential processes involving multiple electron transfer and chemical bond-forming steps. To promote them, various kinds of sophisticated photocatalytic systems have been developed, capable of carrying out sequentially several operations such as light harvesting, charge transfer, transport and storage, substrate binding and product release. Among the systems reported to date are zeolitic materials and heterogeneous metal oxide semiconductors (in particular TiO_2),[14,15] often decorated with supported metal nanoparticles,[16,17] like gold,[18] platinum,[19] nickel[20] and tin,[21] or molecular complexes, like $ReBr(CO)_3(bipy)$,[22] used as co-catalysts; combinations of two different semiconductors to form Z-scheme suspension catalytic systems;[23] homogeneous molecular complexes, such as $[Ir(F\text{-}mppy)_2(dphphen)]^+$[24] and $[Pt(tpy)(phenylacetylide)]^+$,[25] and photosensitizer/catalyst dyads;[26] hybrid and organic polymeric materials such as graphitic carbon nitride ($g\text{-}C_3N_4$),[27] conjugated microporous polymers (CMPs),[28] covalent organic frameworks (COFs)[29,30] and metal-organic layers (MOLs).[31] However, a different solution has also been proposed, based on the use of heterogeneous dye-sensitized photocatalysts (DSP, Figure 1).[32–34]

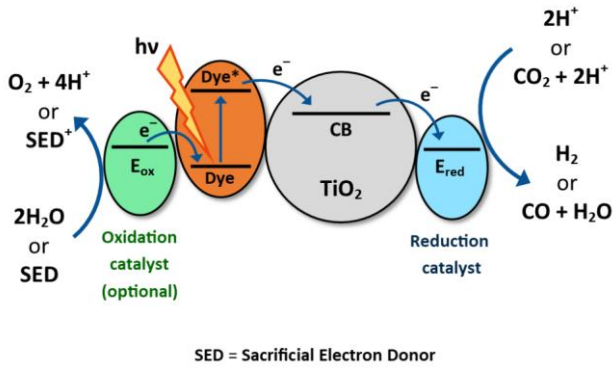

Figure 1. *Schematic working mechanism of a dye-sensitized photocatalytic (DSP) system employing TiO_2 as a semiconductor.*

In a DSP, a molecular dye sensitizer and a catalyst are bridged by co-adsorption on a semiconducting nanoparticle, which acts both as a scaffold and a solid-state electron transfer unit. When hit by light, the sensitizer can absorb photons having energy greater than or equal to its HOMO-LUMO gap, reaching an excited state. If its LUMO level is higher in energy than the conduction band (CB) of the semiconductor, charge separation can take place, eventually followed by electron transfer to the catalyst, which can then promote the desired reduction reaction (leading for example to H_2 or CO formation). The oxidized dye will then be regenerated by electron donation from a suitable reductant (such as water or a sacrificial reagent,

see below), possibly mediated by the presence of another catalyst. Thanks to the employment of sensitizers, it is possible to overcome one of the major drawbacks connected with the use of wide band-gap (≥ 3.0 eV) semiconductors such as TiO_2, namely the lack of light absorption in the visible region.

By modifying independently each part of the ternary DSP system, its optical and redox properties can be tuned, to adapt to the specific conditions of use and the desired reaction to be performed. Sensitizers used in DSP assemblies usually resemble compounds traditionally employed in DSSCs,[3] one of the emerging hybrid organic-inorganic photovoltaic technologies, namely bi- or polypyridine-Ru complexes, metal porphyrins and phthalocyanines,[32] as well as synthetic organic push-pull dyes, whose use is becoming increasingly popular.[35] Among the semiconductors, TiO_2 is largely predominant, but other inorganic species, such as ZnO and $H_4Nb_6O_{17}$, as well as organic materials such as g-C_3N_4[36] have also been reported. Finally, electrocatalysts are often constituted by highly active small metal nanoparticles (Pt, Pd, Au and others), but several authors described also approaches making use of well-defined metal complexes grafted on the semiconductor surface.[33]

In this paper, we will review some selected examples of the use of dye-sensitized photocatalytic systems to promote two main reactions, H_2 generation from water and CO_2 reduction to different C_1-building blocks (in particular CO and formate). Catalyst structure and properties will be discussed, and the relative performances will be assessed, although a direct comparison will often be impossible due to the different conditions used by the various groups in their experiments. Only heterogeneous suspended photocatalytic systems will be considered: readers interested in related approaches based on dye-sensitized photoelectrodes and photoelectrochemical cells are invited to consult some excellent reviews recently published on this subject.[37,38]

2. Hydrogen generation from water

Hydrogen is widely considered the most suitable storage medium for renewable energy since it is an energy dense and carbon neutral fuel, which can be either burned or employed to generate electricity in fuel cells, producing only water as a by-product. In addition, it represents an important feedstock for the modern chemical industry, being used in large scale processes such as the Fischer–Tropsch reaction and ammonia synthesis. Currently, hydrogen is mostly produced by reforming of fossil fuels through various processes (that always generate also carbon dioxide) and used directly on site. A much smaller fraction is produced by water electrolysis, a rather expensive procedure used only when high purity gas is needed.[39,40]

Clearly, a much more sustainable approach to produce hydrogen would be its direct generation from water exploiting a renewable energy source, for example by means of a photocatalytic process (Figure 2a). Indeed, in 1972, the pioneering work of Honda and Fujishima demonstrated the photo-assisted electrochemical water splitting into H_2 and O_2 using a TiO_2 photoanode connected to a platinum cathode in an electrochemical cell.[41] The major disadvantage of such system consisted in the use of a wide band-gap (≥

3.0 eV) semiconductor as the light-harvesting element, limiting absorption and conversion of visible light (λ > 400 nm). Furthermore, an actual photocatalytic procedure for water splitting usually faces several practical problems such as the requirement for a substantial overpotential,[42] the lack of semiconductor materials having both appropriate band energies and stability (Figure 2b), the fast recombination of photogenerated charge carriers, and the facile back reaction between the evolved H_2 and O_2.[43] Consequently, such simple water splitting systems are usually affected by relatively low quantum yields.[15]

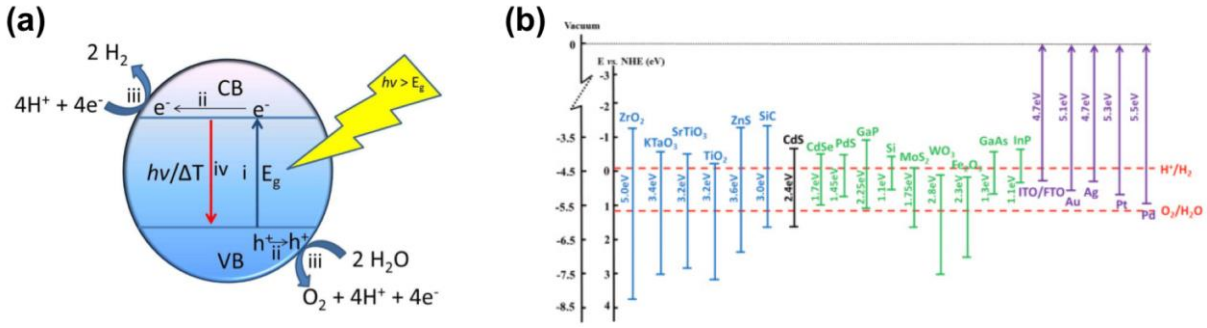

Figure 2. *(a) Photocatalytic water splitting using a single semiconductor. (i) photo-induced charge generation, (ii) charge migration, (iii) photochemical reactions and (iv) charge recombination. Reproduced from ref.*[44] *under the Creative Commons Attribution (CC BY) license. (b) Diagram of energy levels of commonly used semiconductors (blue, black and green), noble metals (purple) and redox potential of splitting water into H_2 and O_2 (red). While some of the materials have not an appropriate band position for water splitting, others, such as CdS, are known to undergo photodegradation under the reaction conditions. Reproduced from ref.*[45] *with permission from Elsevier.*

An effective solution to the issue of insufficient light harvesting in the visible region has been the sensitization of semiconductors with appropriate dyes, able to absorb photons in the desired wavelength range and transfer the resulting photoexcited electrons to the semiconductor.[32–35] On the other hand, the overall productivity of the process has been enhanced by replacing the challenging water oxidation reaction with the reforming of organic sacrificial electron donors (SED),[46] a thermodynamically less demanding process compared with the pure water splitting reaction. Indeed, such compounds present lower oxidation potentials (*e. g.*, for triethanolamine, E° = 0.82 V *vs*. NHE, pH 7; for ascorbic acid, E° < 0.20 V *vs*. NHE, pH 4.5), and are thus able to scavenge h^+ more efficiently than water, enhancing dye regeneration and suppressing charge recombination, while at the same time serving as potential proton sources.[47] The structures of some of the most commonly used SEDs are shown in Figure 3.

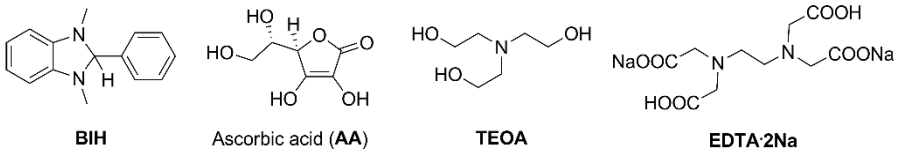

Figure 3. *Structures of some commonly-used sacrificial electron donors (SEDs).*

2.1. Organometallic dyes

Early examples of dye-sensitized photocatalytic hydrogen production were described in the 80s using Ru-bipyridine complexes. The first of these studies was published by Grätzel and co-workers, who reported the use of a bifunctional redox catalyst composed of RuO_2 and Pt supported on nanocrsystalline anatase TiO_2, sensitized by amphiphilic surfactant Ru-bipyridine derivatives bearing alkyl chains of different length ($Ru(bpy)_3^{2+}$ and derivatives, Figure 4a).[48] Surprisingly, the system displayed relatively high activities in overall water splitting under visible light, reaching a maximum quantum yield of approx. 5% for the dodecyl derivative. Based on the experimental observations, the authors proposed for the first time a photochemical mechanism in which adsorption of the sensitizer on the semiconductor surface and its photoexcitation are followed by electron injection into the TiO_2 CB.

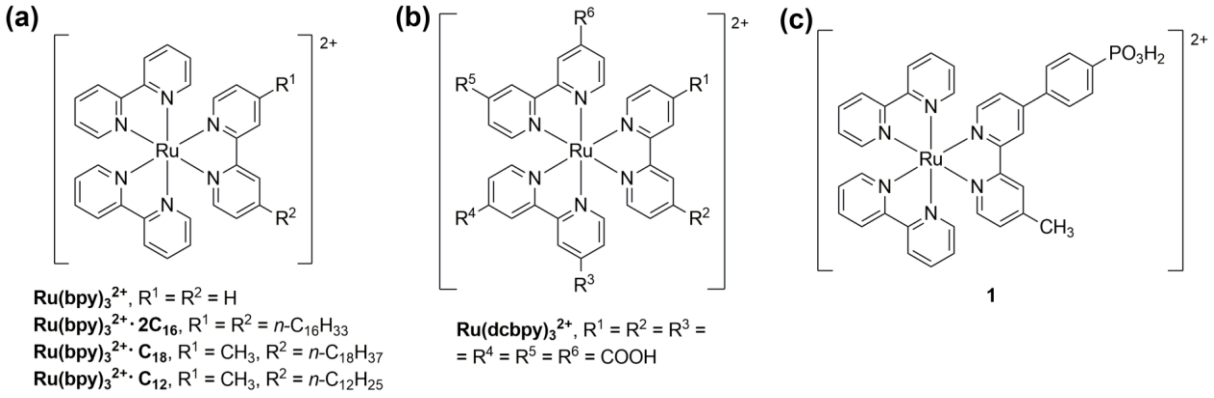

Figure 4. *(a) Amphiphilic Ru-bipyridine complexes decorated with long alkyl chains; (b) fully carboxylated Ru-bipyridine complex; (c) Ru-bipyridine complex decorated with a phosphonic acid anchoring group.*

Subsequently, various other studies on the use of Ru-based sensitizers appeared in the literature, from which it emerged the necessity for the dyes to be strongly adsorbed on the semiconductor to facilitate the charge injection step, due to the typical short lifetime of their excited states.[49–51] Accordingly, in 1986 Furlong and co-workers reported the use of a fully carboxylated Ru-complex, $Ru(dcbpy)_3^{2+}$ (Figure 4b), to sensitize colloidal Pt/TiO_2 towards visible light-mediated H_2 production in the presence of EDTA as a SED.[52] The carboxylic functions of the dye were supposed to act as anchoring groups, enhancing the stability of the dye/semiconductor assembly. The authors found that controlling the pH at which adsorption of the dye and gas evolution took place was the key to maximize anchoring stability and thus catalytic activity. Compared to $Ru(dcbpy)_3^{2+}$, catalysts sensitized with simple $Ru(bpy)_3^{2+}$ provided much worse performances, both at acidic pH with EDTA and at basic pH with triethanolamine (TEOA) as sacrificial agents.

An alternative anchoring group was later identified by Mallouk and co-workers, who used a phosphonate-decorated Ru-bipyridyl complex (**1**, Figure 4c) as a sensitizer for layered metal oxide semiconductors of general formula $K_{4-x}H_xNb_6O_{17}$ decorated with Pt nanoparticles, in the presence of iodide salts as sacrificial donors.[53] The authors found that strong adsorption of the sensitizer on the semiconductor surface allowed

co-adsorption of other species without dye detachment, which was exploited to minimize the rate of back electron transfer while leaving the charge injection and dye regeneration rates unaffected: for example, co-adsorption of anionic polystyrene sulfonate (PSS) led to a 10-fold decrease in the back electron transfer rate, resulting in a 3- to 5-fold increase in the initial hydrogen evolution rate. Subsequently, Choi *et al.* carried out a series of detailed studies comparing the performances of several different photocatalysts composed of Pt/TiO_2 nanoparticles sensitized with ruthenium *tris*-bipyridine complexes carrying a variable number of carboxylate and phosphonate anchoring groups (Figure 5), using EDTA as the sacrificial donor.[54,55] Results showed that, despite the comparable optical properties of the two series of dyes, carboxylate complexes were worse sensitizers for H_2 generation due to their weaker surface anchoring on TiO_2, leading to competition with the reducing agent; conversely, strong adsorption by the phosphonate groups was not hampered by EDTA, resulting in much higher dye loadings. H_2 production was influenced by the number of anchoring groups, with **P2**-TiO_2 catalyst giving much better results than the corresponding **P4**- and **P6**-derivatives. Interestingly, this trend was quite different compared to that observed with the same sensitizers in DSSCs (where **P6** was the best-performing dye),[56] highlighting the influence of the very different interfacial (TiO_2/sensitizer/medium) environments present in the two systems.

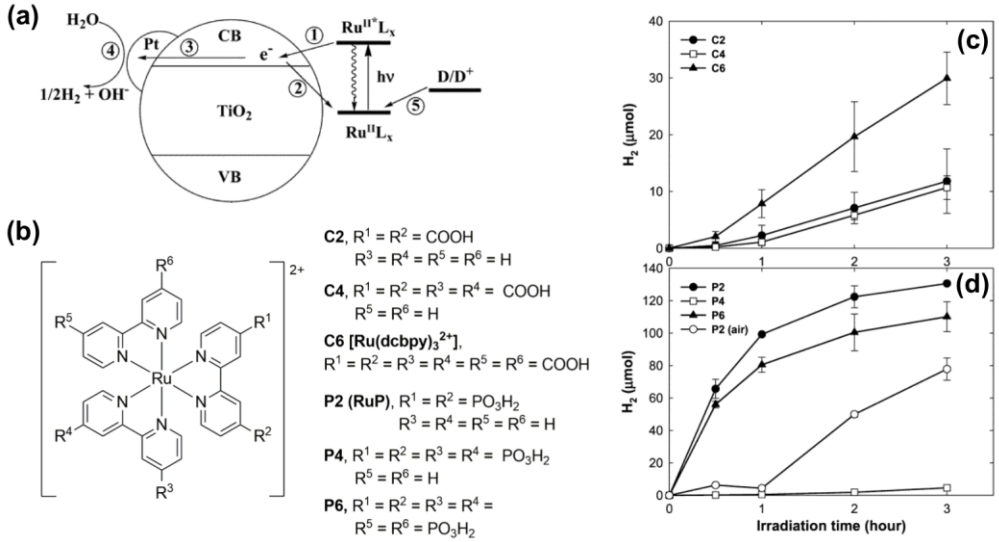

Figure 5. *(a) Mechanism of dye-sensitized hydrogen production with ruthenium complexes; (b) Ru-based sensitizers containing a different number of carboxylate and phosphonate anchoring groups; (c,d) time course of visible light-driven (λ >420 nm) hydrogen evolution reactions in the presence of 10 mM EDTA as SED. Reproduced with permission from ref.*[55]*. © 2006 American Chemical Society.*

More recently, Maeda *et al.* demonstrated that Ru-bipyridyl complexes bearing phosphonate anchoring groups could constitute very active hydrogen generation catalysts also in combination with mixed oxide nanosheets of general formula $HCa_{2-x}Sr_xNb_3O_{10}$ ($0 \le x \le 2$) and $HCa_2Nb_{3-y}Ta_yO_{10}$ ($0 \le y \le 1.5$). They found that

activity was strongly influenced by the E_{CB} position of the semiconductor, and the best results were obtained when a precise matching between the driving forces of electron injection and electron transfer to the nano-Pt catalyst were achieved; the highest activity was provided by an $HCa_2Nb_3O_{10}$ nanosheet, showing a maximum apparent quantum yield of ca. 10% at 460 nm and a turnover number (TON) of ca. 3800 after 20 h.[57]

The group of Reisner investigated the use of P25 (TiO_2) sensitized with **P2** (here called **RuP**) in combination with molecular H_2 evolution catalysts **CoP_{1-2}**, used in place of Pt nanoparticles (Figure 6a,b).[58,59]

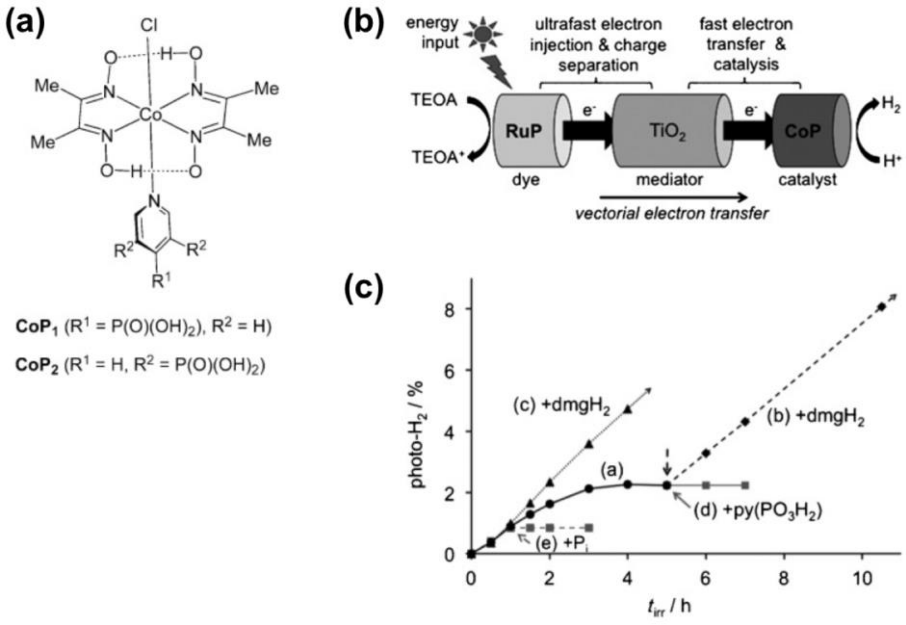

Figure 6. *(a) Structure of **CoP_{1-2}** proton-reduction catalysts; (b) working principle of the heterogeneous photocatalytic systems; (c) hydrogen production experiments under different conditions. In the standard procedure, hydrogen evolution stopped after 5h (trace a); addition of excess ligand ($dmgH_2$), either at the beginning of the experiment or after 5h, completely restored the activity (traces b-c); addition of phosphonate-containing molecules or phosphate buffer, either after 1 or 5h, completely stopped the reaction (traces d-e). Reproduced from ref.* [59] *with permission of Wiley-VCH.*

Such heterogeneous system was found to generate hydrogen efficiently upon visible light irradiation in a pH-neutral aqueous solution at room temperature in the presence of TEOA as the reducing agent. However, a significant drawback was identified in the progressive deactivation of the catalyst, which brought the reaction to a halt after only 5h; the authors found that such phenomenon was due to the dissociation of the dimethylglyoximato (dmg) ligand from the cobalt center, and demonstrated that activity could be completely restored by addition of an excess of $dmgH_2$ (10 equiv) to the exhaust catalyst suspension. Furthermore, it was found that addition of an aqueous phosphate buffer to the catalyst suspension stopped the reaction as well, likely due to the displacement of both **P2** and **CoP** from the semiconductor surface (Figure 6c). Under optimized conditions, a maximum TON > 300 (relative to the cobalt catalyst) could be obtained,

demonstrating that a first-row transition metal complex could serve as an inexpensive alternative to Pt for the photoassisted H_2 evolution reaction on TiO_2.[60]

In a subsequent study, Reisner, Durrant and co-workers studied in more detail the kinetics of the electron transfer processes taking place in their heterogeneous photocatalytic system by means of transient spectroscopy techniques.[61] They found that proton conversion to H_2 requires a two-electron reduction of the **CoP** catalyst from Co^{III} to Co^{I}. While the first electron transfer step from the semiconductor to **CoP** (Co^{III} to Co^{II}) appeared to proceed easily even in the absence of a hole scavenger, the second reduction step (Co^{II} to Co^{I}) was found to be at least 10^5 times slower, suggesting the necessity of efficient hole scavenging and almost complete reduction of all adsorbed **CoP** to Co^{II} for it to proceed. Such considerations highlighted the need for a precise control of charge transfer and charge accumulation processes in such semiconductor/molecular catalyst systems,[62,63] a crucial challenge to be met in order to enhance their performances towards a potential large-scale application.

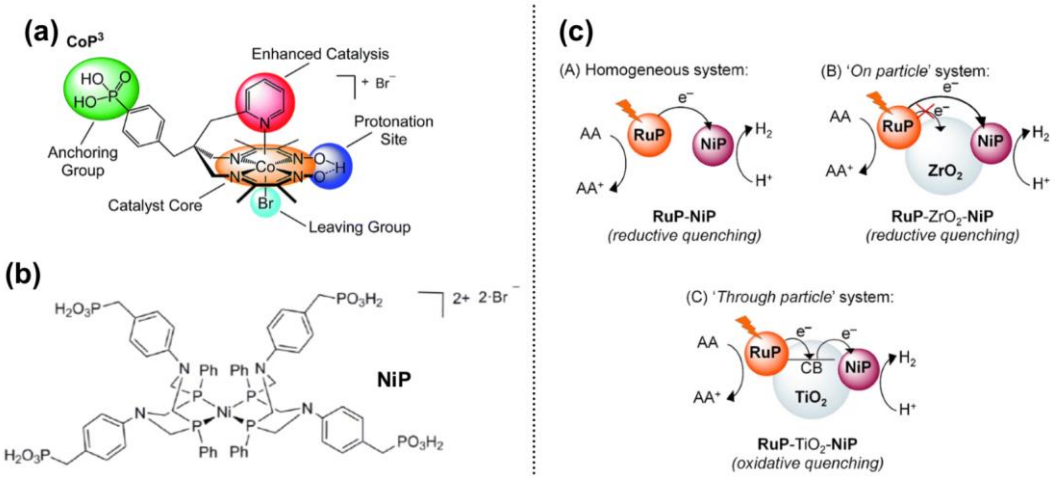

Figure 7. *(a) Structure of **CoP³** proton-reduction catalyst. Reproduced from ref.* [64] *under the Creative Commons Attribution 3.0 Unported licence.; (b) Structure of **NiP** proton-reduction catalyst; (c) Different possible electron transfer pathways for the AA-mediated proton reduction reaction with **RuP** photosensitizer and **NiP** catalyst. Reproduced with permission from ref.* [65]*. © 2014 American Chemical Society.*

To improve the stability of the photocatalytic system and boost his performances, a new Co-based catalyst (named **CoP³**) was later introduced, featuring a rationally-designed diimine-dioxime ligand (Figure 7a).[64] Compared to the complexes shown above, in which the phosphonate anchoring group was attached to the metal through simple coordination *via* a pyridine ring, in **CoP³** both the pyridine moiety (necessary to enhance activity) and the phosphonate group were covalently connected to the equatorial ligand framework, making the whole compound more robust. When used in combination with **RuP**-sensitized TiO_2, the new catalytic system provided different performances depending on the reaction conditions and the SED used. While

reaction with TEOA at neutral pH provided inferior results compared to those obtained with catalyst **CoP$_1$**, a much better result was obtained at pH 4.5 in the presence of ascorbic acid (AA), highlighting the superior robustness of **CoP^3** in acidic conditions. Comparing the **RuP**/TiO_2/**CoP^3** system with the analogous homogenous combination (**RuP** + **CoP^3** dissolved in solution) and the heterogeneous catalyst using ZrO_2 as the semiconductor confirmed that an oxidative quenching, *"through particle"* mechanism was in place, and no direct electron transfer between the sensitizer and the catalyst occurred.

On the contrary, the opposite mechanism was found to be preferred when combining **RuP** with the nickel-based H_2-evolution catalyst **NiP** (Figure 7b-c), featuring a DuBois-type $[Ni(P_2^{R'}N_2^{R''})_2]^{2+}$ core.[65] Indeed, although the **RuP**/TiO_2/**NiP** system was found to be active in the photocatalytic hydrogen production in the presence of AA, a much higher TON was obtained for the homogeneous **RuP**/**NiP** combination, highlighting how a low loading capacity of the materials used and competitive binding of electron donor or electrolyte can still be significant limiting factors for the performances of such hybrid materials.

In recent years, several other reports appeared in the literature describing alternative Ru-based photosensitizers for hydrogen production, mostly aiming at extending the light absorption profile of the resulting catalysts. Modulation of the dyes optical properties was obtained by varying the ligands surrounding the metal center: for example, Pal and co-workers introduced hydroxyquinoline-containing complexes (such as **R1**, Figure 8) demonstrating absorption maxima in solution at around 530 nm with onsets above 700 nm.[66] Later, Peng, Zhang *et al.* employed an hydroxyquinoline ligand to build pincer Ru-complex [Ru(N'NN')(ONO)] (Figure 8), featuring an hydroxyl group as anchoring moiety to the semiconductor. The dye was adsorbed on Pt-loaded TiO_2 and used in the H_2 production reaction under visible light with EDTA as SED, providing a TON of 2166 after 25 h and an excellent apparent quantum yield (AQY) of 27.3% at 420 nm.[67]

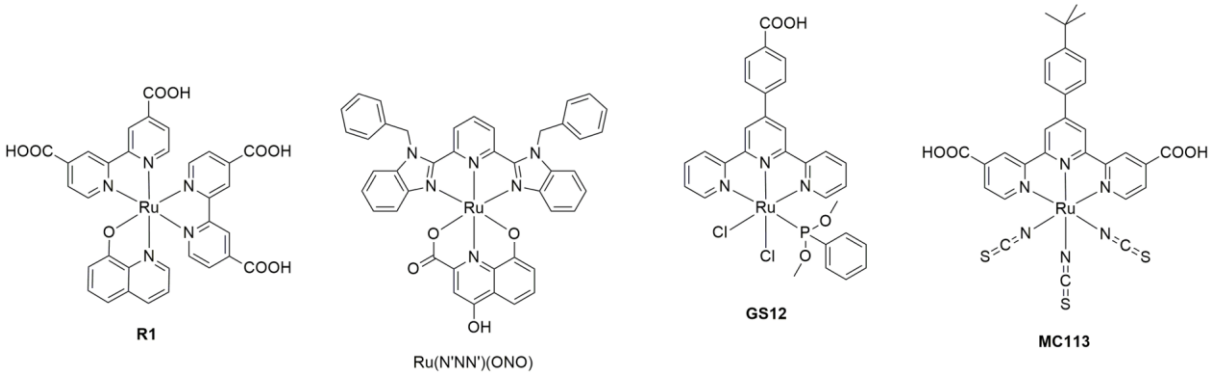

Figure 8. *Chemical structures of Ru-complexes used in photocatalytic hydrogen production.*

A significant extension of the light-absorption range towards longer wavelengths was obtained by adding phosphonite ligands, characterized by low lying π* molecular orbitals and strong donor ability, to the metal coordinating sphere (as in compound **GS12**, Figure 8). The resulting compounds exhibited very broad UV-vis spectra with onsets in the near-infrared region (NIR), albeit with only moderate molar extinction coefficients.

Despite that, high activities were recorded in the H_2 generation reaction in combination with Pt/TiO_2 and TEOA at neutral pH, reaching a maximum TON exceeding 8600 in only 8 h of irradiation (light intensity was around 2 Sun).[68] Modulation of the optical and electrochemical properties of the dyes was also obtained by changing substituents on the structure of terpyridine-thiocyanate ruthenium complexes (such as **MC113**, Figure 8). They presented panchromatic absorption up to 750 nm, accompanied by appropriate HOMO and LUMO positions to ensure smooth electron transfer to the semiconductor and dye regeneration. In the presence of TEOA at neutral pH, **MC113**/TiO_2/Pt afforded a good catalytic activity, with a TON of 2076 after 5 h under visible light irradiation.[69]

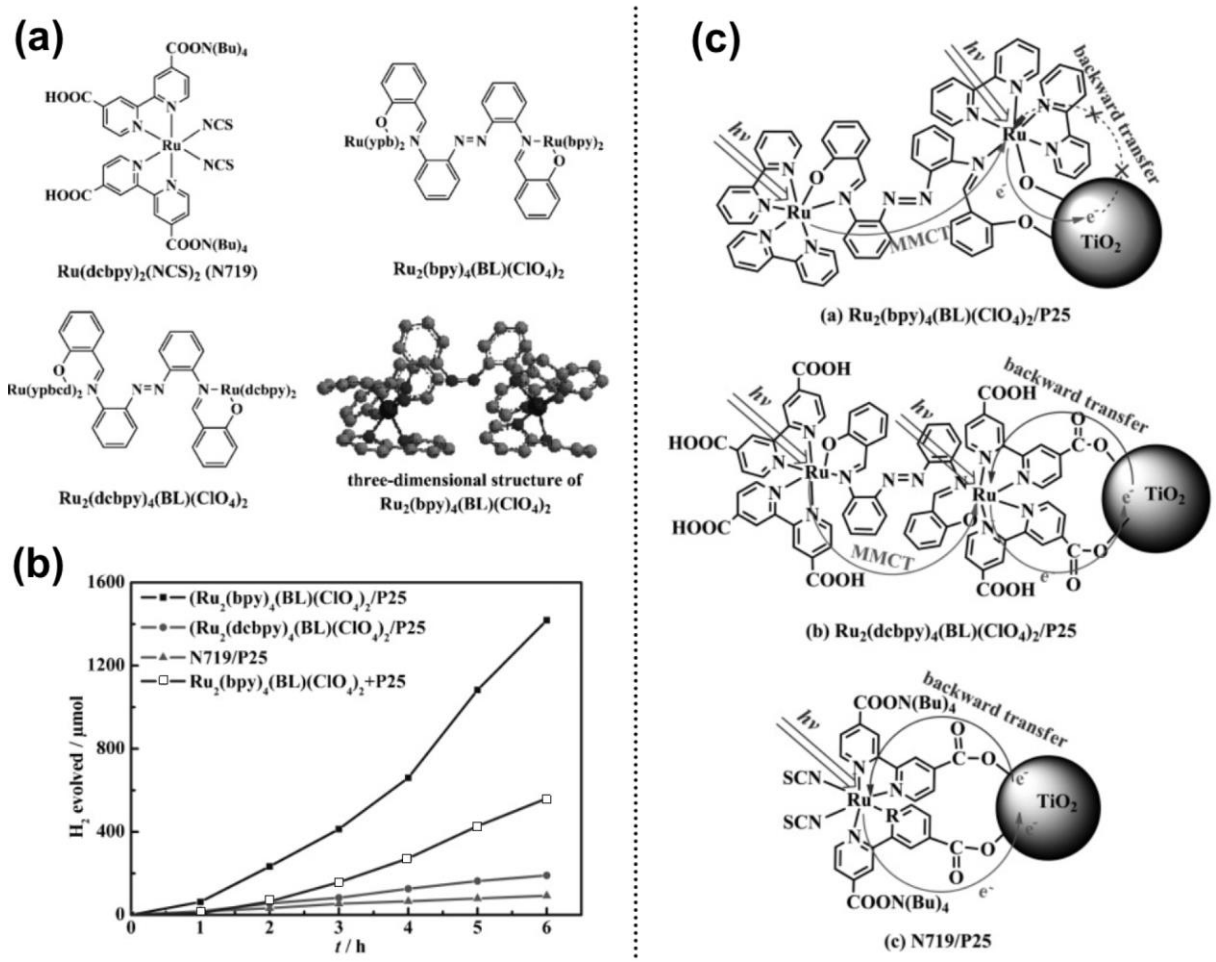

Figure 9. *(a) Structures of the sensitizers tested by Cai, Peng et al.; (b) Hydrogen production experiment using P25 TiO_2 as a semiconductor and TEOA as a SED; (c) Graphical explanation of the better performance displayed by sensitizer [Ru_2(bpy)$_4$(BL)](ClO$_4$)$_2$ compared to the other two dyes. Adapted from ref.*[70] *with permission from Wiley-VCH.*

In apparent contrast with the above reports highlighting the importance of a robust dye attachment to TiO_2, Cai, Peng *et al.* reported an efficient photocatalytic system based on a binuclear Ru-complex loosely attached to the semiconductor.[70] The efficiency of dye [Ru_2(bpy)$_4$(BL)](ClO$_4$)$_2$ (Figure 9a) adsorbed on P25

TiO_2 (without use of any additional catalyst) was compared to those shown by prototypical ruthenium sensitizer **N719** and carboxy-substituted $[Ru_2(dcbpy)_4(BL)](ClO_4)_2$.

Surprisingly, the authors found that the sensitizer devoid of carboxylic anchoring groups provided a much better performance compared to the other two species when used in the presence of TEOA as SED, even when a simple physical mixture with P25 was used (Figure 9b). Such observation was attributed to the specific nature of the sensitizer: on the one hand, the presence of two ruthenium centers allowed an improved charge separation upon photoexcitation thanks to an "antenna effect", driven by a metal-to-metal charge transfer (MMCT) process; on the other, the loose attachment to TiO_2 *via* hydroxyl groups established a dynamic adsorption equilibrium (attachment/detachment of the oxidized sensitizer), minimizing charge recombination compared to the strongly attached dyes (Figure 9c).

2.2. Metal-free Organic Dyes

Another important class of sensitizers employed for photocatalytic hydrogen production are metal free organic dyes; although initial reports concerned the use of fluorescent dyes such as Eosin Y, Rhodamines,[71,72] Rose Bengal[73] and Erythrosin B,[74] more recently research focused on those having a donor- acceptor D-π-A architecture, that was found to be highly versatile and particularly suitable when an efficient charge separation was required. In details, these kind of sensitizers are characterized by the presence of three submolecular units: an electron-donating group (D), a π-spacer (π), and an electron-accepting group (A). Due to the wide diversity of suitable D, A and π fragments, and the availability of efficient methods for their preparation,[75] a huge number of different sensitizers can be accessed, allowing a fine tuning of their chemical, optical, energetic and stability properties.[35]

Of course, sensitizers for hydrogen production need to be designed to work efficiently in water-based media, however most conventional organic dyes are intrinsically hydrophobic and this fact can influence the properties of the dye/TiO_2/water interface, as well as the conformation/aggregation behavior of the dyes adsorbed on the hydrophilic TiO_2 surface, thus having a critical effect on the electron-transfer and chemical processes involved in H_2 generation. In two different papers, Kang and co-workers explored[76][77] the impact of hydrophilic and steric characteristics of organic dyes in sensitized H_2 generation based on Pt/TiO_2 catalysts, using a series of (*E*)-3-[5-(4-(*p*,*p*′-*bis*(R-phenyl)amino)phenyl)-2,2′-bithiophen-2′-yl]-2-cyanoacrylic acid dyes, having hydrophilic or hydrophobic substituent in the dye core. In the first study, parent dye **DH**, having no substituents, was compared with a series of hydrophilic dyes, named **DMOM** and **DEO1-3**, carrying hydrophilic alkoxyalkyl substituents of different length on the donor group. In the second one, the same parent dye (here called **H-D**) was again compared with **DMOM** (here called **MOD**), but also with **PD**, bearing hydrophobic propyl substituent at the diphenylamino end, and **MO4D**, with hydrophilic methoxymethyl substituents at both the outer diphenylamino and inner dithiophene units (Figure 10a).[76][77] It was found that Pt/TiO_2 particles modified with such dyes work as effective catalysts for visible-light-induced H_2 evolution

from aqueous EDTA solutions, revealing a clear dependence on the hydrophilic/hydrophobic character of the substituent R attached to the donor end. Hydrophilic methoxymethyl substitution at the 4,4'-positions of the diphenylamino end group enhances the photosensitization activity compared with the parent **D-H** catalyst, in particular the moderately hydrophilic **DEO1** and **DEO2** catalysts showed substantially higher H_2 generation efficiencies at a low dye adsorption than **D-H**, whereas either slightly hydrophilic **DMOM** or **DEO3,** with the longest ethylene-oxide chains, showed intermediate activity. In contrast, a significant detrimental effect of the hydrophobic propyl substituent is observed in the case of catalyst **PD**, which proved clearly less efficient than the parent compound **HD**. Finally, additional substitution with methoxymethyl groups in the inner dithiophene unit (as in dye **MO4D**) had no particular effect, leading to a slight decrease in H_2 generation (Figure 10b).

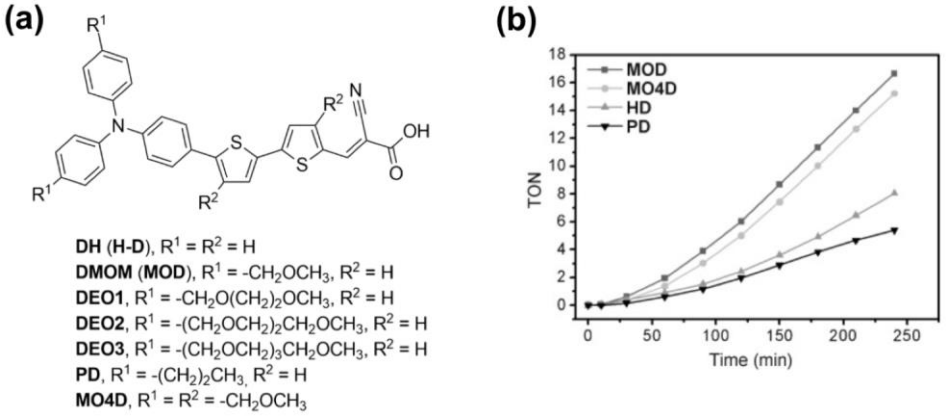

Figure 10. *(a) Chemical structures of the dyes employed by Kang and co-workers; (b) Temporal plots for H_2 generation from water suspensions of the catalysts (1 µmol dye/10 mg Pt/TiO_2) at λ = 420 nm in presence of [EDTA] = 5 mM, pH = 3. Reproduced from ref.*[77] *with permission from Wiley-VCH.*

An in-depth investigation of the different dyes behavior using transient spectroscopy and theoretical calculations led to the conclusions that the different efficiency of the catalysts was the consequence of different solvent reorganization around the hydrophilic or hydrophobic substituent. However, the complex dependence of catalyst activity on the amount of dye fixed to Pt/TiO_2 particles observed in the series **DMOM–DEO3**,[76] being the optimum grafted amounts (μmol/30 mg Pt/TiO_2) considerably different for each dye, namely ~0.15 for **DEO3**, ~0.3 for **DEO1** and **DEO2**, 0.15-0.9 for **DMOM** and ~1.5 for **DH**, was interpreted in terms of the intrinsic enhancement provided by the hydrophilic character being canceled by steric and/or coverage effects. Indeed, a greater hydrophilic character of the substituent coupled with lower steric bulkiness would allow easier access of SED to the radical-cation center localized on the end group of the dye, and thus enhance its reduction compared to charge recombination, leaving greater amounts of long-lived

electrons in the TiO_2 particle. Clearly, the optimization of hydrophilic character coupled with the minimization of steric effects is a key issue for designing organic dyes with high sensitization potential.

The effect of alkyl chains of different length on the efficiency of phenothiazine-based organic dyes (**2-6**) with two anchoring groups at 3,7-positions (Figure 11) was also investigated.[78] The photocatalytic activity of such dyes in aqueous suspension using TEOA as sacrificial reagent, was found significantly high. Furthermore, when compared with similar structures, having a single anchoring group, dyes **3** and **6** showed higher TONs, probably originating from the stability of the corresponding cationic species, as confirmed by their electrochemical behavior. Also in this case, activities of **2–6** were dependent on the kind of alkyl groups attached on nitrogen. As the length of alkyl chains became longer, higher TONs were progressively observed (Figure 11). Thus, among the prepared dyes, **6** with the hexadecyl group on nitrogen gave the best result with 254 mmol H_2 generation after 5 hours, corresponding to a TON of 1026. These results are explained with a positive role played by the longer alkyl chains in maintaining the stability of catalytic cycles, maybe retarding the decomposition of cationic species by blocking the reactions with unfavorable chemical quenchers.[79] Furthermore the alkyl groups on nitrogen can induce a favorable orientation of dyes on TiO_2, which may result in a more efficient electron injection from excited dyes to TiO_2.

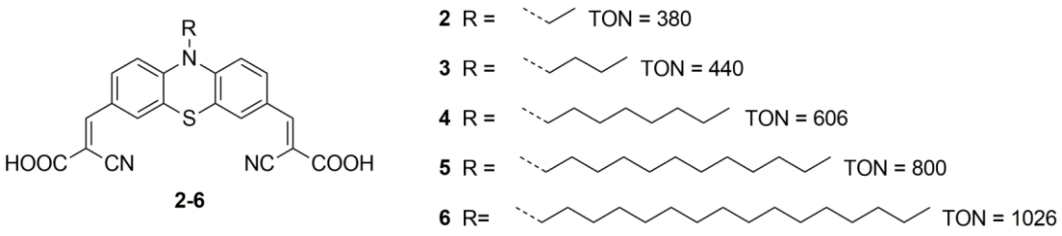

Figure 11. *Structure and photocatalytic performances of phenothiazine-based organic dyes (**2-6**). In the photocatalytic experiments a 200 W Xe lamp was used, cutting light below 420 nm off by means of an optical filter.*

Later, a similar study was conducted on a series of carbazole-based organic dyes bearing 4-alkoxy substituted phenyl rings on nitrogen,[80] to investigate the hydrophobic effect of the different alkyl chains in the dye-sensitized hydrogen production reaction from water (Figure 12a). Despite the electronic properties of the four dyes were found quite similar, once again the hydrogen production yield increased for the dyes with the longest alkoxy chains (**C16**-**C22**), compared to that found for the dye with the shortest substituent (**C1**, Figure 12b). Time-resolved absorption spectra and electrochemical impedance spectroscopy (EIS) analyses suggested that the charge recombination lifetime was dependent on the different alkoxy chain lengths and that **C16** had the longest charge recombination lifetime between the TiO_2 and dye/electrolyte, while **C1** had the shortest. Incident photon-to-electron conversion efficiency (IPCE) spectra confirmed the trend observed in the EIS plots, suggesting that longer alkoxy chain enhanced electron injection from the dye into TiO_2. Furthermore, they reduced dye-packing on the semiconductor surface, enabling easy contact with

the medium at the water/TiO_2 interface: thus, it was shown that hydrogen production could be increased exploiting hydrophobic effects at the interface of the photocatalyst and the water medium. On the other hand, the hydrophobic substituents did not improve the stability of the catalysts, as they did not influence the rate of decomposition of the dye itself and/or its reaction with water.

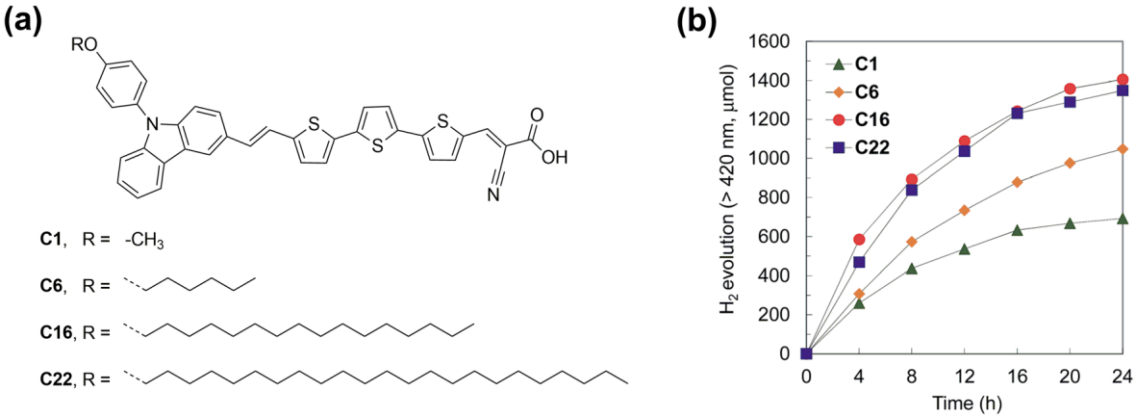

Figure 12. *Structure (a) and photocatalytic activities (b) of dyes **C1**–**C22** in hydrogen production from water. Reaction conditions: 10 vol% aqueous TEOA (10 mL), 33.0 mg dye/TiO_2/Pt catalyst, pH 7.0. Graph reproduced from ref.*[80] *with permission of the Royal Society of Chemistry.*

A more detailed investigation on the nature of hydrophilic substituents was carried out through the synthesis and characterization of three thiophene-based phenothiazine dyes, bearing different substituents on nitrogen.[81] Tris(ethylene glycol) monomethyl ether (TEG) (**PTZ-TEG**), α-D-glucopyranoside (**PTZ-GLU**) and alkyl (n-octyl) (**PTZ-ALK**) derivatives were compared for H_2 production under Vis light (λ > 420 nm) from a triethanolamine/HCl aqueous buffer solution at pH = 7.0 (Figure 13). It was found that **PTZ-GLU** performed twice more efficiently than **PTZ-TEG,** both in terms of evolved H_2 and turnover number, although its activity was comparable to that of **PTZ-ALK**, having opposite physico-chemical properties.

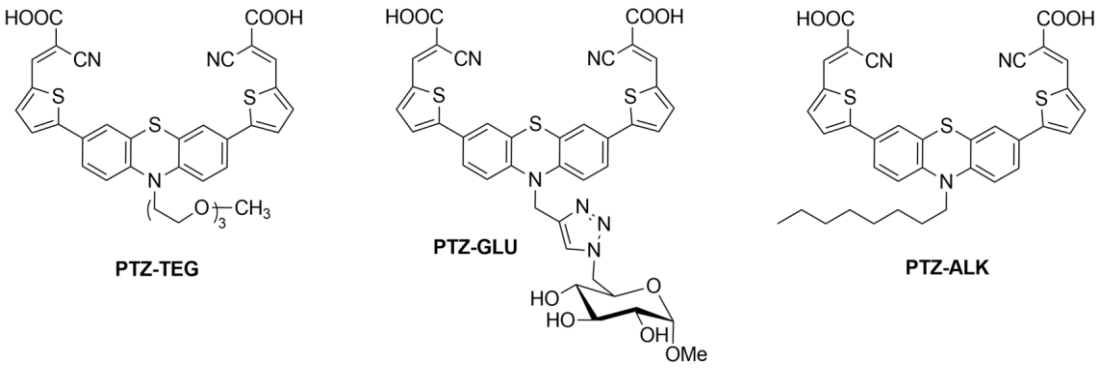

Figure 13. *Structure of thiophene-based phenothiazine dyes with different side-groups.*

Contact angle analysis was used to investigate the hydrophilicity of the catalyst, resulting in a smaller value for **PTZ-GLU**, close to that of bare TiO_2. This led to the conclusion that the introduction of the rigid, bulky and hydrophilic glucose substituent, characterized by lower degrees of freedom as well as the capability of intermolecular self-assembly, clearly improved the wettability of the photocatalyst surface, favoring the interaction with reactants in aqueous solution compared to the TEG chain, especially at lower dye loading. At high loadings, however, the organization of **PTZ-GLU** on the Pt/TiO_2 surface becomes more similar to that of **PTZ-ALK**, with lateral chains mainly avoiding intermolecular quenching, resulting in similar performances.

Such findings support the idea that the sunlight-driven hydrogen generation, both in terms of evolution rates and TON, can be related to the chemical structure of the dyes and to the distinct features of the side functionalities. Along these lines, the same group demonstrated that bidentate molecular sensitizers based on a carbazole scaffold provided much improved performances compared to the analogous phenothiazine and phenoxazine compounds, under the same conditions of the previous study; this result was attributed to the peculiar planar shape of the carbazole ring system, imparting different properties to the dye/semiconductor interface both in terms of dye adsorption and supramolecular organization.[82]

The activity of **PTZ-GLU** dye was later studied in combination both with a glucose-based (glucoronic acid, GLUA) and a conventional (chenodeoxycholic acid, CDCA) co-adsorbent. Results were compared with the activity of the alkyl-derivative **PTZ-ALK**, taken as a reference (Figure 14).[83]

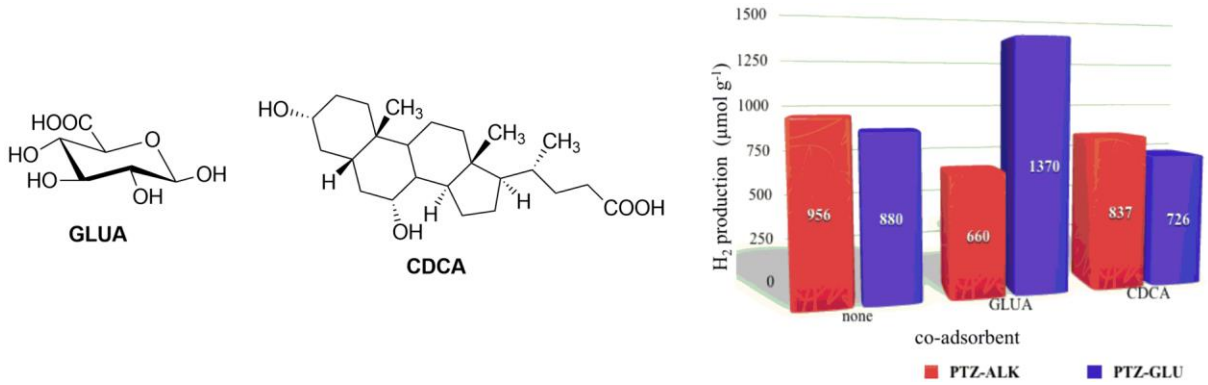

Figure 14. *Structures of the co-adsorbents used in the photocatalytic hydrogen production with dyes **PTZ-GLU** and **PTZ-ALK**, and schematic representation of the results. Graph reproduced with permission from ref.*[83]*. © 2018 American Chemical Society.*

It was found that the combined use of the glucose-based dye and co-adsorbent (**PTZ-GLU**-**GLUA**) afforded enhanced photocatalytic activity in terms of hydrogen generation compared to the absence of co-adsorbents or the presence of a conventional co-adsorbent such as CDCA, less capable of establishing specific directional intermolecular bonds with the dye. Furthermore, the control experiment with **PTZ-ALK** showed that no enhancement could be observed by adding any of the two co-adsorbents compared to the bare dye, as in both cases an improvement was observed only in the presence of higher co-adsorbent−dye ratios (dye

molecules separation by mass effect). These experiments provided the first example of induced intermolecular interactions aimed to enhance photocatalytic H_2 production by modulating the intermolecular arrangement of organic dye sensitizers and co-adsorbents on the photocatalyst surface. DFT simulations on the investigated dye/co-adsorbents systems supported the hypothesis that directional and selective interactions between **PTZ-GLU** and **GLUA** take place on the semiconductor surface, possibly suppressing detrimental dye−dye interactions and leading to improved photocatalytic performances.

The molecular design of sensitizers should also be carefully adjusted depending on the particular SED (and set of conditions) used in the experiments, to yield the best results in the photocatalytic H_2 production. To better understand this point, a series of D–π–A organic dyes with a triarylamine donor unit was synthesized and tested in the photosensitization of Pt/TiO_2.[84] The simple organic dye **D5** was used as a reference and systematically modified by placing hydrophobic alkyl chains on the internal, conjugated section of the sensitizers and/or on their donor part, to obtain insight into the structure–activity and stability relationships (Figure 15).

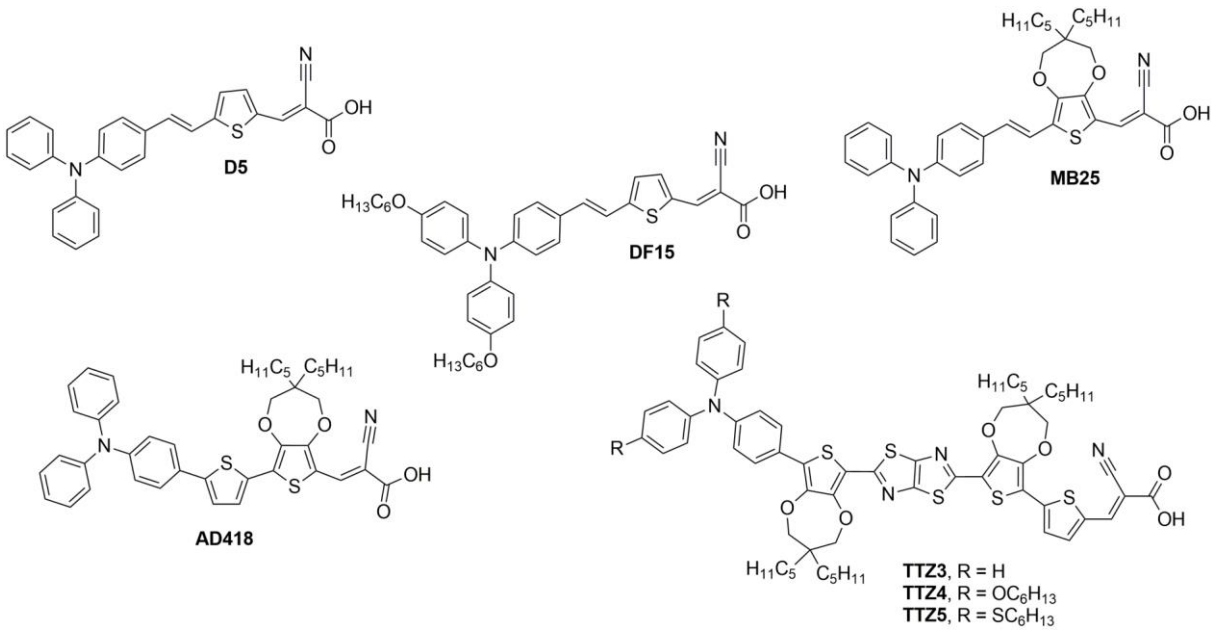

Figure 15. *Structures of organic dyes with different alkyl groups on the terminal or internal parts of the molecular scaffolds.*

The organic dyes were tested using either TEOA or EtOH as SEDs, with the aim to assess the possibility of extending the range of efficient SEDs to renewable alcohols, a potentially significant progress towards the improvement of process sustainability. Results are reported in Table 1.

When employing TEOA, the best result was obtained with sensitizer **AD418**, carrying a propylenedioxythiophene (ProDOT) moiety on the internal scaffold. When compared with the lower activity of compound **DF15** (bearing linear alkoxy substituents on its donor group), this result supported the

hypothesis that placing alkyl chains on the conjugated molecular scaffold could be more effective than inserting them on the donor group, due to a beneficial effect on dye regeneration accompanied by a slowdown of undesired recombination events. On the other hand, thiazolothiazole based dyes, in particular **TTZ4** and **TTZ5**, provided the best activity when using EtOH as the SED. Despite their TONs were lower than those observed when using TEOA, ranging from 99 to 221, (Table 1) such behavior was especially interesting, since it supported for the first time the possibility of using EtOH as sacrificial reagent in a dye-sensitized TiO_2 photocatalytic system. This can be possibly explained considering that **TTZ3-5** dyes have very high molar extinction coefficients and strong light-harvesting capability: such features, coupled with a large driving force for electron injection, could help increase the electron density on TiO_2 under illumination, thereby enhancing H_2 production rates.

Table 1. *Photocatalytic performances of the dye/Pt/TiO_2 catalysts in H_2 production with TEOA or EtOH as SED under irradiation with visible light (λ > 420 nm).*

Dye	SED	H_2 amount[a] [μmol g^{-1}]	TON[b]
D5	TEOA	1884	397
	EtOH	-	-
DF15	TEOA	2371	474
	EtOH	-	-
MB25	TEOA	2846	569
	EtOH	-	-
AD418	TEOA	4359	**872**
	EtOH	403	81
TTZ3	TEOA	1424	285
	EtOH	493	99
TTZ4	TEOA	1550	310
	EtOH	1102	220
TTZ5	TEOA	3432	686
	EtOH	1105	**221**

[a] Overall H_2 amount produced after 20 h of irradiation per gram of catalyst. [b] TON=(2×H_2 total amount after 20 h of irradiation)/(dye loading).

In a subsequent study, the combination of organic sensitizers with different crystalline forms of TiO_2 was investigated.[85] The dyes used in this case featured a dithienosilole (DTS) core, a triarylamine donor and a

cyanoacrylic acid acceptor, and were decorated with alkyl chains in different positions of the molecular scaffold (Figure 16a). It was found that, when combined with different TiO_2 polymorphs, namely P25 (80/20 mixture of anatase and rutile) and brookite, in the presence of TEOA as electron donor, the best performing dye (**OB2**) provided different results in the visible light-driven hydrogen production reaction. In particular, the catalytic system based on brookite proved more active, giving higher H_2 amounts and TON values compared to the other, especially at lower dye loadings (Figure 16b). This observation was explained considering the lower reactivity of conduction band electrons of brookite compared to anatase,[86] in turn resulting in a reduced rate of charge recombination, in agreement with previous studies conducted on DSSCs.[87] Remarkably, the **OB2**/brookite/Pt system showed also a very high stability, as proven by the fact that the photocatalytic reaction still proceeded after 170 h under continuous illumination (Figure 16c), resulting in a TON of 4201.

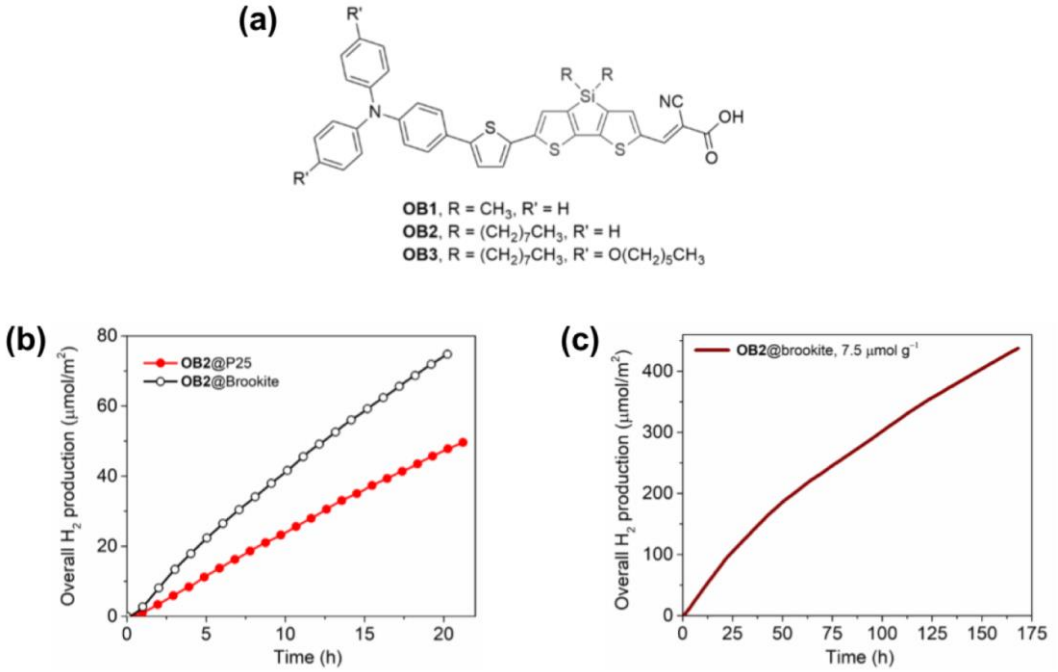

Figure 16. *(a) Structure of DTS-based sensitizers **OB1-3**; (b) Hydrogen production per catalyst surface area of **OB2**-sensitized P25/Pt (red circles) and brookite/Pt (black hollow circles) over 20 h visible light irradiation (λ > 420 nm, light intensity ~1080 W m^{-2}, dye loading, 10 μmol·g^{-1}); c) Hydrogen production relative to surface area of **OB2**@ brookite/Pt catalyst over 170 h of visible light irradiation. All experiments were performed with TEOA as SED. Reproduced with permission from ref.* [85]*. © 2019 American Chemical Society.*

A rare example of full water splitting achieved with a dye-sensitized photocatalytic system was reported by Abe and co-workers, who employed two different catalysts for the oxidation and reduction semi-reactions, organized in a Z-scheme.[88] The hydrogen production reaction was promoted by crystals of ion exchangeable layered niobium oxide ($H_4Nb_6O_{17}$) decorated with Pt nanoparticles and sensitized with coumarin-based or oligothiophene dyes (NKX and MK series, Figure 17); the water oxidation catalyst was constituted by WO_3

nanoparticles coloaded with Pt and IrO_2, while a triiodide/iodide (I_3^-/I^-) redox couple was employed as a shuttle electron mediator between the two composites, according to the cartoon shown in Figure 17a.

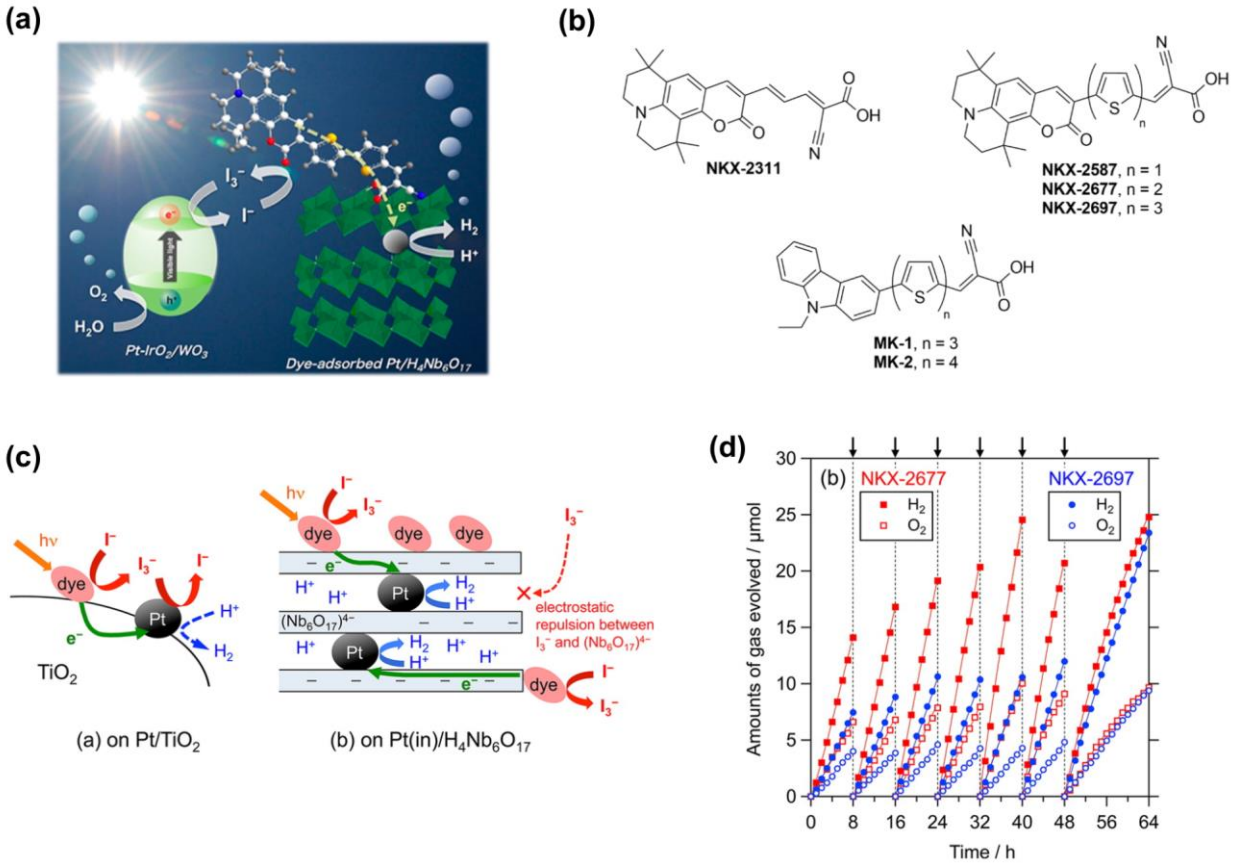

Figure 17. *(a) Mechanism of dye-sensitized water splitting with a Z-scheme photocatalytic system; (b) Structures of the coumarin and oligothiophene dyes; (c) Conceptual scheme illustrating suppression of backward reaction using nanostructured layered semiconductors; (d) Time courses of H_2 and O_2 evolution using a mixture of dye-adsorbed $Pt/H_4Nb_6O_{17}$ (50 mg) and IrO_2-Pt/WO_3 (100 mg) suspended in 5 mM KI aqueous solution (pH ~ 4.5) under visible light. Arrows indicate evacuation of gas phase. Reproduced with permission from ref.* [88]*. © 2013 American Chemical Society.*

Importantly, it was found that under these conditions H_2 evolution was completely suppressed when using the typical Pt/TiO_2 system, which did not occur with the $Pt/H_4Nb_6O_{17}$ material. This was attributed to the preferential reduction of I_3^- on the titania catalyst surface, inhibiting the proton reduction reaction; in the case of layered $H_4Nb_6O_{17}$, instead, such parasitic process could not take place since I_3^- anions are unable to access the Pt particles inside due to the electrostatic repulsion between them and the negatively charged $(Nb_6O_{17})^{4-}$ layers, allowing to employ the collected electrons solely to produce hydrogen (Figure 17c). The best results were obtained with coumarin dyes **NKX-2677** and **NKX-2697**, which were able to produce a substantial quantity of H_2 and O_2 (TON max. in the 317-513 range) in a nearly stoichiometric ratio with good stability, the system being still active after 64 h under illumination (Figure 17d). This result highlighted the need for a good charge separation upon photoexcitation of the dye to improve electron injection and reduce

recombination, allowed by the presence of a large number of conjugated thiophene rings placed between the donor and the acceptor unit.

3. Photocatalytic Reduction of CO_2

The solar-driven CO_2 reduction entails two undeniable benefits, namely the production of energy-rich fuels and chemicals such as carbon monoxide, formic acid, ethylene and methane, and the valorization of atmospheric carbon dioxide, focusing onto the goal of converting a waste into a renewable resource. Three different types of dye-sensitized photocatalysts have been used for carbon dioxide reduction: (a) TiO_2 is functionalized with two distinct units, a photosensitizer and a reduction catalyst (Dye/TiO_2/Cat), (b) a carrier supports both the photosensitizer and the reduction catalyst (Dye/Supp/Cat), (c) a supramolecular adduct formed by a dye covalently bound to a reduction catalyst is adsorbed on semiconducting nanoparticles (ScNPs/Dye-Cat).

3.1. Type (a): Dye/TiO_2/Cat

The first photosensitization of a TiO_2 surface with a dye for CO_2 reduction was reported by Uner *et al.*[89] in 2007. Thick and thin films of TiO_2, coated on hollow glass beads and containing platinum as catalyst, were photosensitized with **Ru(bpy)$_3^{2+}$**, **BrGly** and **BrAsp** as dyes (Figure 4 and Figure 18).

The dye-sensitized TiO_2 surfaces were used to initiate the photoreduction of carbon dioxide to methane with water in the gas phase. Under UV illumination, the presence of the dye was detrimental for CH_4 production (around 8 *vs.* 2 μmoles methane/g-cat in 180 hours), probably because the electron-hole pairs generated in the bulk of TiO_2 were quenched at the dye-semiconductor surface. On the other hand, under visible illumination bare Pt/TiO_2 showed no photocatalytic activity, while dye-sensitized Pt/TiO_2 films revealed to be active in CO_2 reduction, even if the amounts of photo-generated methane were one order of magnitude lower than under UV irradiation (around 0.8 μmoles methane/g-cat in 180 hours with **BrAsp**/TiO_2/Pt catalyst). The same approach was employed by Wu *et al*.[90] who ran the same gas-phase reaction using as photocatalyst optical fibers coated with TiO_2 doped with copper (0.5 wt%) and iron (0.5 wt%) and then colored with **N3**[91] (Figure 18), a dye intensively studied as photosensitizer in DSSCs. Using a solar concentrator (average natural light intensity of 20 mW cm^{-2}) the photocatalyst reduced carbon dioxide to methane with a production rate of 0.617 μmoles/g-cat h, a two-fold increase in comparison to the same catalyst without **N3**. More recently, Long *et al.*[92] performed the same gas-phase CO_2 reduction to methane in the presence of liquid water, using TiO_2 grafted with ruthenocene [$(C_5H_5)_2Ru$]. Their best photocatalyst, a (C_5H_5)-RuH-O-TiO_2 hybrid with a 0.6 wt% Ru content, was able to produce CH_4 with a maximal rate of 44.0 μL g^{-1} h^{-1}, 7-fold higher than the efficiency of the reference counterpart, prepared by covalent bonding of ligands of a Ru complex to the surface of TiO_2.

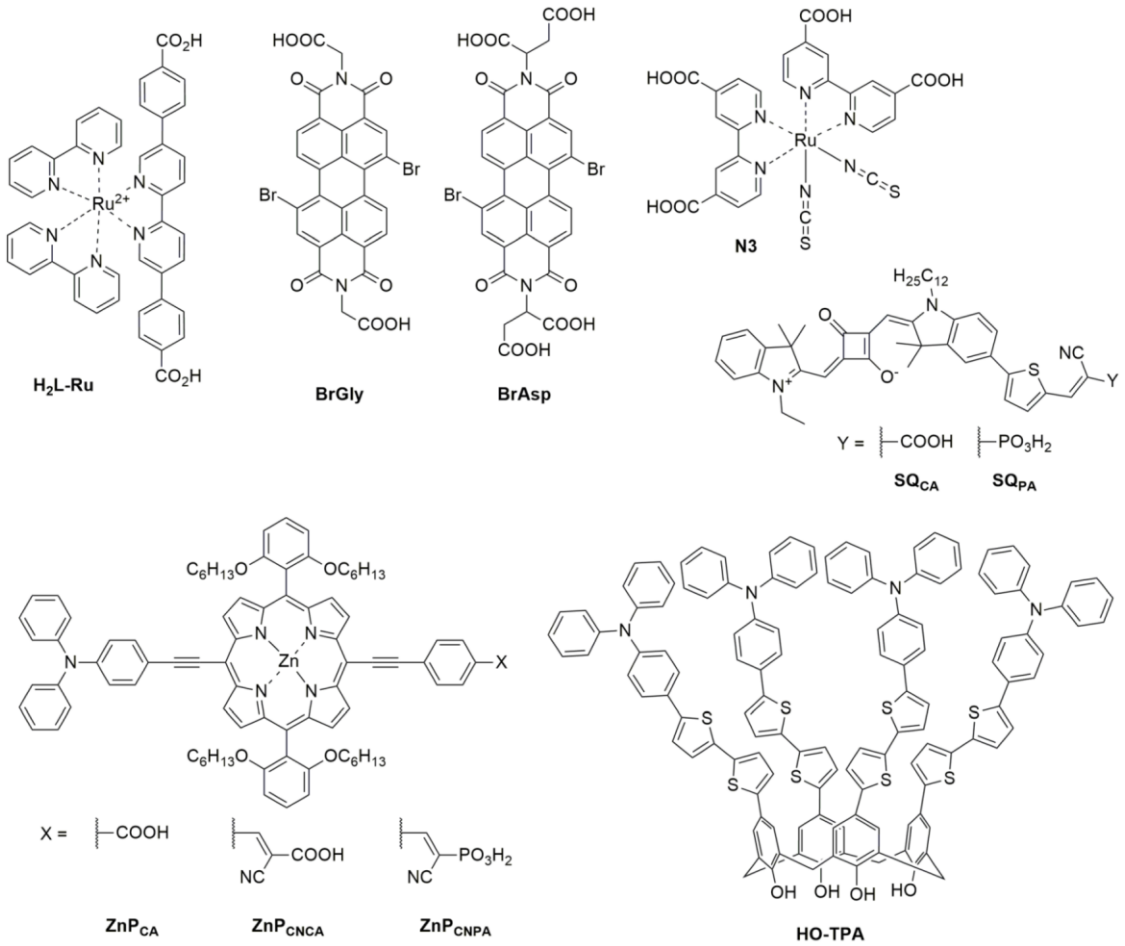

Figure 18. *Structures of organic and organometallic photosensitizers used in CO_2 reduction.*

In recent years, a well-defined configuration has also been developed to carry out CO_2 reductions in organic suspensions (Dye/TiO_2/Cat – Figure 19), especially thanks to the contribution of Kang and coworkers, who introduced many changes, such as the immobilization of organometallic complexes, previously used for CO_2 reduction in homogeneous solutions, on TiO_2 nanoparticles and the employment of SEDs different than water. In such a system, the dye anchored on the TiO_2 harvests solar light, the photoexcited electrons are injected into the conduction band of the semiconducting oxide and then transferred to the metal complex (Cat), which reduces the substrate. On the other side, the dye is restored in the reduced form through oxidation of the SED.

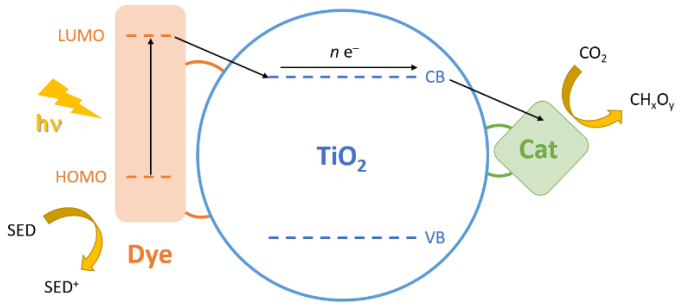

Figure 19. *Depiction of electron flow in the solar-driven CO_2 reduction on a Dye/TiO_2/Cat system.*

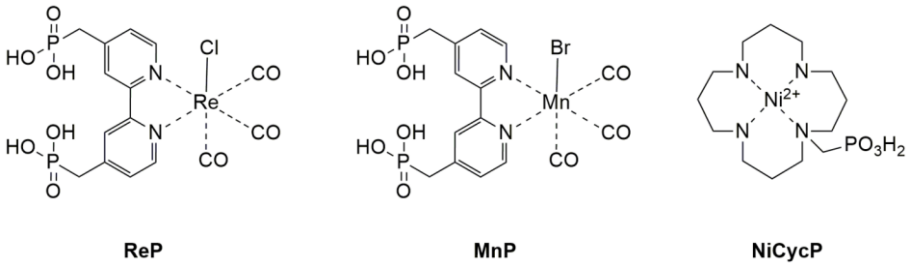

Figure 20. *Structures of organometallic reduction catalysts.*

The first tested photocatalyst[93,94] was composed by TiO_2 nanoparticles decorated with the simple organic dye **DMOM** (Figure 10) and the Re(I) complex **ReP** (Figure 20), a proper derivative of the $(bpy)Re(CO)_3Cl$ complex reported by Lehn *et al.*[95] in 1983. The **DMOM**/TiO_2/**ReP** adduct was assembled dipping the TiO_2 nanoparticles (Hombikat UV-100) first in a dye solution and then in a **ReP**-containing solution. The photocatalyst was suspended in a solution of donor **BIH** (Figure 3) in CO_2-saturated *N*,*N*-DMF with a 3% addition of water, which was fundamental to get a proper alignment of the energetic levels, as depicted in Figure 19. The choice of *N*,*N*-DMF instead of water was mainly due to the higher solubility of CO_2 in this solvent and the decreased proton concentration, which minimizes the competitive hydrogen evolution. After irradiation with a Xenon lamp (450 W), the photocatalytic system was able to provide a steady and selective production of CO, reaching a TON_{CO} equal to 570 in 30 hours of experiment.

A different class of dyes, able to exploit the near-IR region of the solar spectrum, have also been tested in combination with the same TiO_2 particles, reduction catalyst and SED under lower energy irradiation (> 500 nm) using a LED lamp (60 W). Among the **ZnP** series of porphyrins[96] (Figure 18), the adduct with $\mathbf{ZnP_{CA}}$ showed the best activity, but survived less than 42 hours, while the $\mathbf{ZnP_{CNPA}}$-based catalytic system showed a stable CO production during 92 h of experiment and a TON_{CO} of ≈ 800. Squaraine-dyes $\mathbf{SQ_{CA}}$ and $\mathbf{SQ_{PA}}$ (Figure 18) have been also tested under lower energy irradiation,[97] but an inefficient CO production was observed because of a substantial photobleaching of the dye due to the operating conditions in *N*,*N*-DMF solution. Despite that, even the photodegraded $\mathbf{SQ_{PA}}$, whose structure was not determined, was found to work as an actual photosensitizer, giving a moderate TON of ≈ 165 for 70 h under high energy illumination (> 400 nm). Fortunately, the degradation of the dye was rapid only in organic environment. Indeed, $\mathbf{SQ_{PA}}$/TiO_2 nanoparticles containing Pt were efficient photocatalysts in H_2 production: working in aqueous environment and using ascorbic acid as SED, no photobleaching of the dye was observed and TON_{H2} up to 4200 was measured. Using dye **DH** (Figure 10) and **BIH** as SED, different reduction catalysts have been tested in order to prepare products other than CO. Anchoring both catalysts **ReP** (Figure 20) and $\mathbf{CoP_1}$ (Figure 6a), Kang *et al.* were able to produce both CO and H_2 (syngas), and the ratio between the two gases was adjustable by varying either the amount of water in the solvent mixture (0-20%) or the molar ratio of the two catalysts.[98] By contrast, anchoring of **MnP** catalyst (Figure 20) allowed to obtain formate as the main product with a

$TON_{formate}$ of ≈ 250 after 23 h of irradiation (> 400 nm, 60 W).[99] Selectivity of the system towards the formate production was a matter of Mn concentration on the TiO_2 surface, since loading of the catalyst higher than 0.1 μmol favored the formation of Mn-Mn dimers, which are more selective towards the formation of carbon monoxide instead of formate.

A different kind of dye was used by Liu, Su and coworkers, who introduced four light-harvesting units in a calix[4]arene scaffold, decorated with four –OH groups (**HO-TPA**, Figure 18) required to create a very strong binding with TiO_2.[100] **ReP** (Figure 20) was chosen as the catalyst and anchored to the **HO-TPA**/TiO_2 system, while a mixture of **BIH** and TEOA was found to be the best performing combination of SEDs. Under illumination with a 300 W Xenon lamp (> 420 nm), CO was produced as the unique product with a TON_{CO} equal to 534 for 26 hours and no photobleaching of the dye was observed. Moreover, the same photocatalytic system with platinum instead of **ReP** and TEOA as the only SED was able to produce hydrogen too, giving a TON of 6417 for 75 hours.

3.2. Type (b): Dye/Supp/Cat

Some examples of the second photocatalytic configuration have been also reported. In this case (Dye/Supp/Cat – Figure 21), TiO_2 is replaced by a support which is not directly involved in the electron transfer mechanism. The role of the support is to place the photosensitizer and the reduction catalyst close enough to make the direct electron transfer between the two species possible. Cowan *et al.* reported an example where the support was made of ZrO_2 nanoparticles, **RuP** (Figure 5b) was the dye and **NiCycP** (Figure 20) the catalyst.[101] Since electron injection from the dye excited state into ZrO_2 cannot occur, the catalytic cycle shows some slight differences compared to the previous case. First, **RuP** is photoexcited (**RuP***), then reduced to Ru^{I} (**RuP**$^{-}$) by ascorbic acid used as the SED: **RuP**$^{-}$ is actually the species able to transfer one electron to **NiCycP**, which can perform a reduction reaction. Unfortunately, the selectivity of the reductive process was quite low (H_2/CO ≈ 4/1), with a TON of 4.8 for CO production, still a higher value than that reported for a solution-based approach using **NiCycP** (≈ 0.1).

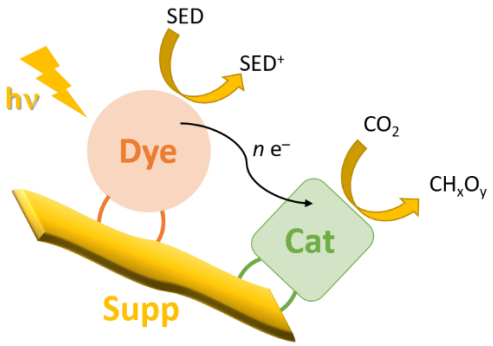

Figure 21. *Illustration of mechanism of a solar-driven CO_2 reduction on the Dye/Supp/Cat system.*

A completely different approach was chosen by Lin *et al.*, who synthesized, starting from $HfCl_4$ and **H_2L-Ru** (Figure 18), a photosensitizing metal-organic layer (Hf_{12}-Ru) containing Hf_{12} secondary building units and **$[Ru(bpy)_3]^{2+}$** linkers to form an infinite 2D network.[31] Hf_{12}-Ru was then metalated with $Re(CO)_5Cl$ or $Mn(CO)_5Br$, that acted as reduction catalysts. The Re-containing photocatalyst proved to be more active and more selective than the Mn-containing one, in the reduction of CO_2 to CO using **BIH** as SED, reaching a turnover number of 8613 under artificial visible light (> 400 nm) in five days, and of 670 under sunlight in one day. Mechanistic studies proved that the excited Hf_{12}-Ru was reduced by **BIH** to generate $[Hf_{12}\text{-}Ru]^-$ which had the right potential to transfer one electron to the Re or Mn-center. Analogously, Zhang and coworkers supported the **H_2L-Ru** dye and Co^{2+} ions on a Zr-based metal-organic framework, called UiO-67(bpydc).[102] Irradiating for 16 hours a CO_2-saturated solution of **TEOA** in CH_3CN/H_2O in the presence of the Ru/Co-containing molecular organic framework (MOF), a high evolution yield of 1.36×10^4 μmol/g of syngas was achieved. The proportion H_2/CO was adjusted to 2/1 varying the ratio between Ru and Co in the material. Authors claimed that the transfer of electrons occurred from the excited state of the Ru-complex to the cobalt catalyst, which used them to produce syngas, while TEOA regenerated the oxidized ruthenium center.

Covalent organic frameworks (COFs) have been used as carriers as well. Bi *et al.* prepared a cobalt-modified covalent triazine-based framework (Co/CTFs) through polymerization of 1,4-dicyanobenzene in acid environment and impregnation with $CoCl_2$, which was tested for CO evolution.[103] Authors stated that, because of the chemical nature of the carrier, CTF was not an innocent support, since its basic character enhanced the CO_2 capture capacity. Moreover, in this case, the dye, **$[Ru(bpy)_3]^{2+}$** (Figure 4), was not anchored to the surface of the material, but was simply confined in the porous structure of the organic framework. In the presence of TEOA as SED and under visible light irradiation (> 420 nm), the CO production rate was up to 50 μmol g^{-1} h^{-1}.

3.3. Type (c): ScNPs/Dye-Cat

The third approach to photocatalysts (ScNPs/Dye-Cat – Figure 22) differs from the othersin that the dye and the reduction catalyst are covalently linked by an alkyl chain. This supramolecular assembly (Dye-Cat), containing a photosensitizer unit and a catalyst unit, is anchored to particles of a semiconducting material (ScNPs), which is also able to absorb visible light. In this configuration, the irradiated light must be absorbed by both ScNP and the photosensitizer unit, in fact the energetic levels of the two species are aligned in the way that photoexcited electrons in the conduction band of the ScNP can be transferred only to the excited or oxidized photosensitizer unit, but not to the ground state. Then, an intramolecular electron transfer from the excited state of the photosensitizer unit to the catalyst unit occurs in order to have CO_2 reduction, while the photogenerated holes in the valence band of the ScNPs can oxidize the sacrificial electron donor.

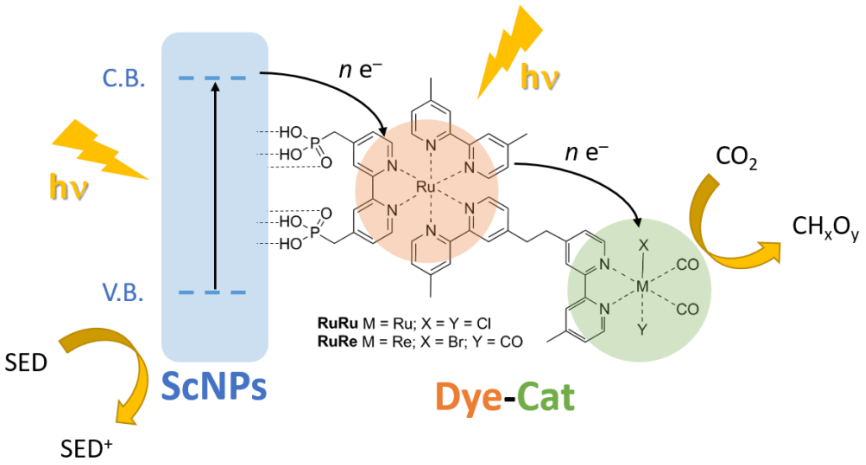

Figure 22. *Depiction of electron flow in the solar-driven CO_2 reduction on the ScNPs/Dye-Cat system.*

The field is dominated by the remarkable work developed by Maeda, Ishitani and coworkers. In 2013 the group reported a ScNPs/Dye-Cat system for the photocatalytic CO_2 reduction, using TaON particles loaded with 1 wt% metallic silver as ScNPs and a supramolecule composed by two ruthenium complexes (**RuRu** – Figure 22) linked by an ethyl bridge as the Dye-Cat.[104] The photocatalytic experiment was run irradiating a suspension of the catalyst in methanol with a 500-W Hg lamp in the visible region (> 400 nm) for 15 hours: formic acid was obtained as the sole CO_2 reduction product (TON = 41), but together with a comparable amount of hydrogen. Traces of CO were also detected, but the authors demonstrated that it was mainly originated from the detachment of CO ligands from the catalyst unit. The other reaction product is formaldehyde, deriving from the oxidation of methanol by the photogenerated holes in the TaON valence band. The presence of silver was essential since, in its absence, the HCOOH production was ten times smaller. Authors stated that silver increases the efficiency in methanol oxidation and plays the role of an electron supply, accelerating the electron transfer to the photosensitized unit.

The same binuclear complex **RuRu** was also exploited using a different semiconductor made of mesoporous graphitic carbon nitride (C_3N_4) modified with silver nanoparticles.[105] This material enhanced the catalytic performances of the system and a very high HCOOH selectivity > 99% and a TON_{HCOOH} up to 3110 were reached in 5 hours, using a solution of TEOA in *N*,*N*-dimethylacetamide (DMAc) as SED under visible light irradiation. Longer experiments of 48 hours were run under the same conditions and an impressive TON_{HCOOH} > 33000 was obtained, even if with a lower selectivity (≈ 87%). Authors demonstrated that this photocatalytic system could operate in water too,[106] using **EDTA·2Na** (Figure 3) as sacrificial electron donor in conjunction with K_2CO_3 (0.1 M) as additive. Basic conditions, in fact, increased the production of formate (TON > 2000) and the selectivity (> 90%), without accelerating the desorption of **RuRu** from the Ag/C_3N_4 system. Despite that, after prolonged times of irradiation, the decomposition of the Ru complexes occurred, leading to a decline in CO_2 reduction.

A different Dye-Cat supramolecule (**RuRe** – Figure 22) was also investigated by the same authors for the CO production.[107] Again, the semiconducting material was made of C_3N_4 nanosheets modified with 5-10 nm TiO_2 nanoparticles and the experiments were run using a TEOA solution in *N,N*-dimethylacetamide (DMAc) as SED and irradiating over 400 nm for 20 hours. Under these conditions, CO was produced with a good selectivity (≈ 80%) and a TON_{CO} of 73, which was about 4 times greater than that obtained using the sample without TiO_2. According to the authors, the presence of TiO_2 nanoparticles minimized the electron-hole recombination in C_3N_4, since the photoexcited electrons in C_3N_4 were pushed to move to TiO_2 by the difference in the conduction band energy between the two materials, resulting in a prolonged lifetime of the electrons. Moreover, TiO_2 resulted to be a stronger binding site for **RuRe**: for this reason, a decrease of the desorption ratio in TiO_2/C_3N_4 system was achieved. A similar modification of C_3N_4 surface with SiO_2 nanoparticles was also investigated, but, despite the amount of adsorbed **RuRe** was initially much higher, the CO production dropped after only 5 hours because of an undesired desorption of the Dye-Cat supramolecule from the surface of SiO_2/C_3N_4 in the operating conditions.[108]

Summary and Outlook

In recent years, solar fuels production by means of dye-sensitized photocatalytic systems (DSP) has witnessed tremendous advancements, and several ingenious systems for the generation of both H_2 and CO_2-derived building blocks (such as CO and formate) have been described in the literature. Compared to other heterogeneous and homogeneous systems, DSP offer the possibility to combine the compounds performing the different functions (light absorption, charge transport, redox chemistry) in a rapid and straightforward way, mostly by simple self-assembly on the surface of organic or inorganic semiconductors or supports. In addition, use of nanostructured semiconductors allows to efficiently accumulate multiple and long-lived electrons, making it possible to transfer them to the catalysts to carry out the required reduction reactions.

Despite all these advantages, DSP can still be affected by significant drawbacks, such as the limited efficiency, the imperfect selectivity (e. g. in the reduction of CO_2, where different C_1 compounds can be obtained alongside with H_2) and the insufficient stability, often resulting from decomposition of the photosensitizer or alteration of the catalyst complex. In addition, molecular dyes (and organic dyes in particular) are often characterized by narrow absorption profiles compared to those of inorganic semiconductors, which limits the light harvesting capability of the system. Finally, as explained in the paragraphs above, most DSP systems currently need a sacrificial reagent to work, and the use of water as terminal reducing agent both in the photocatalytic hydrogen production and CO_2 reduction is very rare.

To overcome this issues, a more precise understanding of the photoexcitation and charge-transfer processes taking place at the various interfaces of the photocatalytic system (e. g. between dye and semiconductor) will be mandatory, in order to enhance their efficiency and minimize energy losses. This kind of studies will require application of advanced spectroscopic techniques, able to elucidate the kinetics of

electron transfer events in hybrid catalytic systems, such as transient absorption spectroscopy (TAS) and time-resolved fluorescence spectroscopy, as well as employment of suitable computational protocols to describe the electronic properties of the compounds ground- and excited states. From the synthetic point of view, it will be necessary to develop sensitizers characterized by improved anchoring stability and superior robustness under irradiation, to avoid photobleaching phenomena and increase the durability of the photocatalytic assembly. Furthermore, tuning of their electronic properties will allow to harvest light in a wider region of the visible spectrum, improving overall efficiencies; alternatively, improvement of the light harvesting ability shall be pursued by applying co-sensitization sensitization strategies, or exploiting energy transfer processes (*e g.* FRET) between different chromophores.

Finally, appropriate strategies should be further elaborated to allow the use of water as reducing agent, thus achieving real artificial photosynthetic processes, for example by coupling the photosensitizers to efficient water-oxidation catalysts on the semiconductor surface, as already demonstrated in photoelectrochemical cells.[38] Alternatively, proton or carbon dioxide reduction could be coupled with oxidation of selected organic substrates, providing access to high added value chemicals by means of light-driven, sustainable chemical processes.[109]

References

[1] *BP Statistical Review of World Energy*, BP P.L.C., **2019**.

[2] *REthinking Energy 2017: Accelerating the Global Energy Transformation*, International Renewable Energy Agency (IRENA), **2017**.

[3] A. Hagfeldt, G. Boschloo, L. Sun, L. Kloo, H. Pettersson, *Chem. Rev.* **2010**, *110*, 6595–6663.

[4] A. Le Donne, A. Scaccabarozzi, S. Tombolato, S. Marchionna, P. Garattini, B. Vodopivec, M. Acciarri, S. Binetti, *ISRN Renew. Energy* **2013**, 830731.

[5] H. Huang, J. Huang, Eds. , *Organic and Hybrid Solar Cells*, Springer International Publishing, **2014**.

[6] J.-P. Correa-Baena, A. Abate, M. Saliba, W. Tress, T. Jesper Jacobsson, M. Grätzel, A. Hagfeldt, *Energy Environ. Sci.* **2017**, *10*, 710–727.

[7] F. Gao, L. J. A. Koster, T.-Q. Nguyen, N. Stingelin, *Adv. Energy Mater.* **2018**, *8*, 1802706.

[8] *Key World Energy Statistics*, International Energy Agency (IEA), **2018**.

[9] N. Armaroli, V. Balzani, *Chem. – A Eur. J.* **2016**, *22*, 32–57.

[10] T. R. Cook, D. K. Dogutan, S. Y. Reece, Y. Surendranath, T. S. Teets, D. G. Nocera, *Chem. Rev.* **2010**, *110*, 6474–6502.

[11] V. Balzani, A. Credi, M. Venturi, *ChemSusChem* **2008**, *1*, 26–58.

[12] J. Mao, K. Li, T. Peng, *Catal. Sci. Technol.* **2013**, *3*, 2481–2498.

[13] D. Kim, K. K. Sakimoto, D. Hong, P. Yang, *Angew. Chemie Int. Ed.* **2015**, *54*, 3259–3266.

[14] E. V Kondratenko, G. Mul, J. Baltrusaitis, G. O. Larrazábal, J. Pérez-Ramírez, *Energy Environ. Sci.*

2013, *6*, 3112–3135.

[15] Z. Wang, C. Li, K. Domen, *Chem. Soc. Rev.* **2019**, *48*, 2109–2125.

[16] A. Dhakshinamoorthy, S. Navalon, A. Corma, H. Garcia, *Energy Environ. Sci.* **2012**, *5*, 9217–9233.

[17] J. Zhao, B. Liu, L. Meng, S. He, R. Yuan, Y. Hou, Z. Ding, H. Lin, Z. Zhang, X. Wang, et al., *Appl. Catal. B Environ.* **2019**, *256*, 117823.

[18] J. Long, H. Chang, Q. Gu, J. Xu, L. Fan, S. Wang, Y. Zhou, W. Wei, L. Huang, X. Wang, et al., *Energy Environ. Sci.* **2014**, *7*, 973–977.

[19] Y. Zhou, Z. Zhang, Z. Fang, M. Qiu, L. Ling, J. Long, L. Chen, Y. Tong, W. Su, Y. Zhang, et al., *Proc. Natl. Acad. Sci. U. S. A.* **2019**, *116*, 10232–10237.

[20] L. Fan, J. Long, Q. Gu, H. Huang, H. Lin, X. Wang, *J. Catal.* **2014**, *320*, 147–159.

[21] H. Huang, J. Lin, L. Fan, X. Wang, X. Fu, J. Long, *J. Phys. Chem. C* **2015**, *119*, 10478–10492.

[22] C. D. Windle, E. Pastor, A. Reynal, A. C. Whitwood, Y. Vaynzof, J. R. Durrant, R. N. Perutz, E. Reisner, *Chem. – A Eur. J.* **2015**, *21*, 3746–3754.

[23] K. Maeda, *ACS Catal.* **2013**, *3*, 1486–1503.

[24] J. I. Goldsmith, W. R. Hudson, M. S. Lowry, T. H. Anderson, S. Bernhard, *J. Am. Chem. Soc.* **2005**, *127*, 7502–7510.

[25] X. Wang, S. Goeb, Z. Ji, N. A. Pogulaichenko, F. N. Castellano, *Inorg. Chem.* **2011**, *50*, 705–707.

[26] S. Berardi, S. Drouet, L. Francàs, C. Gimbert-Suriñach, M. Guttentag, C. Richmond, T. Stoll, A. Llobet, *Chem. Soc. Rev.* **2014**, *43*, 7501–7519.

[27] G. Zhang, Z.-A. Lan, L. Lin, S. Lin, X. Wang, *Chem. Sci.* **2016**, *7*, 3062–3066.

[28] C. Yang, B. C. Ma, L. Zhang, S. Lin, S. Ghasimi, K. Landfester, K. A. I. Zhang, X. Wang, *Angew. Chemie Int. Ed.* **2016**, *55*, 9202–9206.

[29] X. Wang, L. Chen, S. Y. Chong, M. A. Little, Y. Wu, W. H. Zhu, R. Clowes, Y. Yan, M. A. Zwijnenburg, R. S. Sprick, et al., *Nat. Chem.* **2018**, *10*, 1180–1189.

[30] J. Ming, A. Liu, J. Zhao, P. Zhang, H. Huang, H. Lin, Z. Xu, X. Zhang, X. Wang, J. Hofkens, et al., **2019**, 1–6.

[31] G. Lan, Z. Li, S. S. Veroneau, Y. Y. Zhu, Z. Xu, C. Wang, W. Lin, *J. Am. Chem. Soc.* **2018**, *140*, 12369–12373.

[32] X. Zhang, T. Peng, S. Song, *J. Mater. Chem. A* **2016**, *4*, 2365–2402.

[33] J. Willkomm, K. L. Orchard, A. Reynal, E. Pastor, J. R. Durrant, E. Reisner, *Chem. Soc. Rev.* **2016**, *45*, 9–23.

[34] M. Watanabe, *Sci. Technol. Adv. Mater.* **2017**, *18*, 705–723.

[35] B. Cecconi, N. Manfredi, T. Montini, P. Fornasiero, A. Abbotto, *European J. Org. Chem.* **2016**, *2016*, 5194–5215.

[36] J. Zhu, P. Xiao, H. Li, S. A. C. Carabineiro, *ACS Appl. Mater. Interfaces* **2014**, *6*, 16449–16465.

[37] Z. Yu, F. Li, L. Sun, *Energy Environ. Sci.* **2015**, *8*, 760–775.

[38] F. Li, H. Yang, W. Li, L. Sun, *Joule* **2018**, *2*, 36–60.

[39] N. Armaroli, V. Balzani, *ChemSusChem* **2011**, *4*, 21–36.

[40] S. Z. Baykara, *Int. J. Hydrogen Energy* **2018**, *43*, 10605–10614.

[41] A. Fujishima, K. Honda, *Nature* **1972**, *238*, 37–38.

[42] J. Li, N. Wu, *Catal. Sci. Technol.* **2015**, *5*, 1360–1384.

[43] S. Chen, T. Takata, K. Domen, *Nat. Rev. Mater.* **2017**, *2*, 17050.

[44] J. Albero, D. Mateo, H. García, *Molecules* **2019**, *24*, 906.

[45] Y. Zhao, N. Hoivik, K. Wang, *Nano Energy* **2016**, *30*, 728–744.

[46] Y. Pellegrin, F. Odobel, *Comptes Rendus Chim.* **2017**, *20*, 283–295.

[47] N. Luo, Z. Jiang, H. Shi, F. Cao, T. Xiao, P. P. Edwards, *Int. J. Hydrogen Energy* **2009**, *34*, 125–129.

[48] E. Borgarello, J. Kiwi, E. Pelizzetti, M. Visca, M. Grätzel, *Nature* **1981**, *289*, 158–160.

[49] D. Duonghong, E. Borgarello, M. Graetzel, *J. Am. Chem. Soc.* **1981**, *103*, 4685–4690.

[50] E. Borgarello, J. Kiwi, E. Pelizzetti, M. Visca, M. Graetzel, *J. Am. Chem. Soc.* **1981**, *103*, 6324–6329.

[51] V. H. Houlding, M. Gratzel, *J. Am. Chem. Soc.* **1983**, *105*, 5695–5696.

[52] D. N. Furlong, D. Wells, W. H. F. Sasse, *J. Phys. Chem.* **1986**, *90*, 1107–1115.

[53] G. B. Saupe, T. E. Mallouk, W. Kim, R. H. Schmehl, *J. Phys. Chem. B* **1997**, *101*, 2508–2513.

[54] E. Bae, W. Choi, J. Park, H. S. Shin, S. Bin Kim, J. S. Lee, *J. Phys. Chem. B* **2004**, *108*, 14093–14101.

[55] E. Bae, W. Choi, *J. Phys. Chem. B* **2006**, *110*, 14792–14799.

[56] H. Park, E. Bae, J.-J. Lee, J. Park, W. Choi, *J. Phys. Chem. B* **2006**, *110*, 8740–8749.

[57] K. Maeda, G. Sahara, M. Eguchi, O. Ishitani, *ACS Catal.* **2015**, *5*, 1700–1707.

[58] F. Lakadamyali, E. Reisner, *Chem. Commun.* **2011**, *47*, 1695–1697.

[59] F. Lakadamyali, A. Reynal, M. Kato, J. R. Durrant, E. Reisner, *Chem. – A Eur. J.* **2012**, *18*, 15464–15475.

[60] J. Willkomm, E. Reisner, *Bull. Japan Soc. Coord. Chem.* **2018**, *71*, 18–29.

[61] A. Reynal, F. Lakadamyali, M. A. Gross, E. Reisner, J. R. Durrant, *Energy Environ. Sci.* **2013**, *6*, 3291–3300.

[62] E. Sundin, M. Abrahamsson, *Chem. Commun.* **2018**, *54*, 5289–5298.

[63] V. Saavedra Becerril, E. Sundin, M. Abrahamsson, *J. Phys. Chem. C* **2018**, *122*, 25822–25828.

[64] J. Willkomm, N. M. Muresan, E. Reisner, *Chem. Sci.* **2015**, *6*, 2727–2736.

[65] M. A. Gross, A. Reynal, J. R. Durrant, E. Reisner, *J. Am. Chem. Soc.* **2014**, *136*, 356–366.

[66] I. Mondal, A. Tiwari, R. Ghosh, U. Pal, *RSC Adv.* **2016**, *6*, 41165–41172.

[67] C. Zhuang, J. Wang, S. Zhou, T. Peng, J. Zhang, *ChemPhotoChem* **2018**, *2*, 765–772.

[68] T. Swetha, I. Mondal, K. Bhanuprakash, U. Pal, S. P. Singh, *ACS Appl. Mater. Interfaces* **2015**, *7*, 19635–19642.

[69] G. Koyyada, N. S. Pilli, J. H. Jung, K. K. Mandari, B. Shanigaram, M. Chandrasekharam, *Int. J. Hydrogen Energy* **2018**, *43*, 6963–6976.

[70] X. Zhang, U. Veikko, J. Mao, P. Cai, T. Peng, *Chem. – A Eur. J.* **2012**, *18*, 12103–12111.

[71] D. Chatterjee, *Catal. Commun.* **2010**, *11*, 336–339.

[72] R. Abe, K. Hara, K. Sayama, K. Domen, H. Arakawa, *J. Photochem. Photobiol. A Chem.* **2000**, *137*, 63–69.

[73] Z. Xiaojie, J. Zhiliang, L. Yuexiang, L. Shuben, L. Gongxuan, *J. Phys. Chem. C* **2009**, *113*, 2630–2635.

[74] P. Zhang, T. Song, T. Wang, H. Zeng, *RSC Adv.* **2017**, *7*, 17873–17881.

[75] L. Zani, A. Dessì, D. Franchi, M. Calamante, G. Reginato, A. Mordini, *Coord. Chem. Rev.* **2019**, *392*, 177–236.

[76] S. H. Lee, Y. Park, K. R. Wee, H. J. Son, D. W. Cho, C. Pac, W. Choi, S. O. Kang, *Org. Lett.* **2010**, *12*, 460–463.

[77] W. S. Han, K. R. Wee, H. Y. Kim, C. Pac, Y. Nabetani, D. Yamamoto, T. Shimada, H. Inoue, H. Choi, K. Cho, et al., *Chem. - A Eur. J.* **2012**, *18*, 15368–15381.

[78] J. Lee, J. Kwak, K. C. Ko, J. H. Park, J. H. Ko, N. Park, E. Kim, D. H. Ryu, T. K. Ahn, J. Y. Lee, et al., *Chem. Commun.* **2012**, *48*, 11431–11433.

[79] J. E. Kroeze, N. Hirata, S. Koops, M. K. Nazeeruddin, L. Schmidt-Mende, M. Grätzel, J. R. Durrant, *J. Am. Chem. Soc.* **2006**, *128*, 16376–16383.

[80] M. Watanabe, H. Hagiwara, Y. Ogata, A. Staykov, S. R. Bishop, N. H. Perry, Y. J. Chang, S. Ida, K. Tanaka, T. Ishihara, *J. Mater. Chem. A* **2015**, *3*, 21713–21721.

[81] N. Manfredi, B. Cecconi, V. Calabrese, A. Minotti, F. Peri, R. Ruffo, M. Monai, I. Romero-Ocaña, T. Montini, P. Fornasiero, et al., *Chem. Commun.* **2016**, *52*, 6977–6980.

[82] N. Manfredi, M. Monai, T. Montini, M. Salamone, R. Ruffo, P. Fornasiero, A. Abbotto, *Sustain. Energy Fuels* **2017**, *1*, 694–698.

[83] N. Manfredi, M. Monai, T. Montini, F. Peri, F. De Angelis, P. Fornasiero, A. Abbotto, *ACS Energy Lett.* **2018**, *3*, 85–91.

[84] A. Dessì, M. Monai, M. Bessi, T. Montini, M. Calamante, A. Mordini, G. Reginato, C. Trono, P. Fornasiero, L. Zani, *ChemSusChem* **2018**, *11*, 793–805.

[85] O. Bettucci, T. Skaltsas, M. Calamante, A. Dessì, M. Bartolini, A. Sinicropi, J. Filippi, G. Reginato, A. Mordini, P. Fornasiero, et al., *ACS Appl. Energy Mater.* **2019**, *2*, 5600–5612.

[86] J. J. M. Vequizo, H. Matsunaga, T. Ishiku, S. Kamimura, T. Ohno, A. Yamakata, *ACS Catal.* **2017**, *7*, 2644–2651.

[87] Y. Kusumawati, M. Hosni, M. A. Martoprawiro, S. Cassaignon, T. Pauporté, *J. Phys. Chem. C* **2014**, *118*, 23459–23467.

[88] R. Abe, K. Shinmei, N. Koumura, K. Hara, B. Ohtani, *J. Am. Chem. Soc.* **2013**, *135*, 16872–16884.

[89] O. Ozcan, F. Yukruk, E. U. Akkaya, D. Uner, *Appl. Catal. B Environ.* **2007**, *71*, 291–297.

[90] T. V. Nguyen, J. C. S. Wu, C. H. Chiou, *Catal. Commun.* **2008**, *9*, 2073–2076.

[91] M. K. Nazeeruddin, A. Kay, I. Rodicio, R. Humphry-Baker, E. Müller, P. Liska, N. Vlachopoulos, M. Grätzel, *J. Am. Chem. Soc.* **1993**, *115*, 6382–6390.

[92] H. Huang, J. Lin, G. Zhu, Y. Weng, X. Wang, X. Fu, J. Long, *Angew. Chemie - Int. Ed.* **2016**, *55*, 8314–8318.

[93] E. G. Ha, J. A. Chang, S. M. Byun, C. Pac, D. M. Jang, J. Park, S. O. Kang, *Chem. Commun.* **2014**, *50*, 4462–4464.

[94] D. Il Won, J. S. Lee, J. M. Ji, W. J. Jung, H. J. Son, C. Pac, S. O. Kang, *J. Am. Chem. Soc.* **2015**, *137*, 13679–13690.

[95] J. Hawecker, J.-M. Lehn, R. Ziessel, *J. Chem. Soc. Chem. Commun.* **1983**, 536–538.

[96] D. Il Won, J. S. Lee, Q. Ba, Y. J. Cho, H. Y. Cheong, S. Choi, C. H. Kim, H. J. Son, C. Pac, S. O. Kang, *ACS Catal.* **2018**, *8*, 1018–1030.

[97] M. Jo, S. Choi, J. H. Jo, S.-Y. Kim, P. S. Kim, C. H. Kim, H.-J. Son, C. Pac, S. O. Kang, *ACS Omega* **2019**, *4*, 14272–14283.

[98] J. S. Lee, D. Il Won, W. J. Jung, H. J. Son, C. Pac, S. O. Kang, *Angew. Chemie - Int. Ed.* **2017**, *56*, 976–980.

[99] S. J. Woo, S. Choi, S. Y. Kim, P. S. Kim, J. H. Jo, C. H. Kim, H. J. Son, C. Pac, S. O. Kang, *ACS Catal.* **2019**, *9*, 2580–2593.

[100] Y.-F. Chen, J.-F. Huang, M.-H. Shen, J.-M. Liu, L.-B. Huang, Y.-H. Zhong, S. Qin, J. Guo, C.-Y. Su, *J. Mater. Chem. A* **2019**, *7*, 19852–19861.

[101] G. Neri, M. Forster, J. J. Walsh, C. M. Robertson, T. J. Whittles, P. Farràs, A. J. Cowan, *Chem. Commun.* **2016**, *52*, 14200–14203.

[102] M. Liu, Y. F. Mu, S. Yao, S. Guo, X. W. Guo, Z. M. Zhang, T. B. Lu, *Appl. Catal. B Environ.* **2019**, *245*, 496–501.

[103] J. Bi, B. Xu, L. Sun, H. Huang, S. Fang, L. Li, L. Wu, *Chempluschem* **2019**, *84*, 1149–1154.

[104] K. Sekizawa, K. Maeda, K. Domen, K. Koike, O. Ishitani, *J. Am. Chem. Soc.* **2013**, *135*, 4596–4599.

[105] R. Kuriki, H. Matsunaga, T. Nakashima, K. Wada, A. Yamakata, O. Ishitani, K. Maeda, *J. Am. Chem. Soc.* **2016**, *138*, 5159–5170.

[106] R. Kuriki, M. Yamamoto, K. Higuchi, Y. Yamamoto, M. Akatsuka, D. Lu, S. Yagi, T. Yoshida, O. Ishitani, K. Maeda, *Angew. Chemie - Int. Ed.* **2017**, *56*, 4867–4871.

[107] K. Wada, C. S. K. Ranasinghe, R. Kuriki, A. Yamakata, O. Ishitani, K. Maeda, *ACS Appl. Mater. Interfaces* **2017**, *9*, 23869–23877.

[108] K. Wada, M. Eguchi, O. Ishitani, K. Maeda, *ChemSusChem* **2017**, *10*, 287–295.

[109] X. Lang, X. Chen, J. Zhao, *Chem. Soc. Rev.* **2014**, *43*, 473–486.

Graphical Abstract

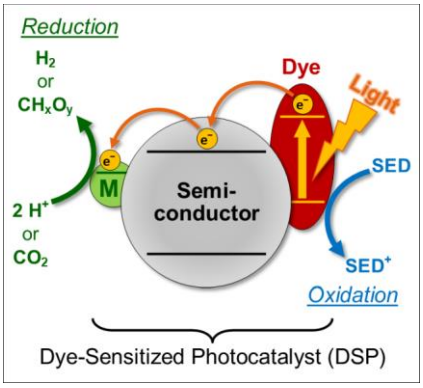

Dye-sensitized photocatalysts (DSP) are currently among the most promising systems employed for the production of solar fuels. In this review, selected examples of the use of DSP for H^+ and/or CO_2 reduction will be discussed, highlighting how materials properties and catalyst composition can affect the efficiency of such "artificial photosynthetic" processes.

Key Topic

Artificial Photosyntesis

Keywords

Photocatalysis;

Dye Sensitization;

Hydrogen;

Solar Fuels;

Organometallics.

Research group Twitter account: LEaF Lab (@LabLeaf)

Corresponding Authors Biographies

Gianna Reginato graduated in chemistry at the University of Florence in 1983. After a post-doctoral experience at Basel University, Switzerland under the supervision of Prof. Bernd Giese, she was appointed Researcher at CNR in Florence. Since 2001 she is Senior Researcher at the Institute of Organometallic Compounds (CNR-ICCOM) Sesto Fiorentino, Italy. Her research interest is in synthetic organic chemistry, especially in the field of metal mediated processes (silicon and tin derivatives, organo and metallocuprates, cross-coupling reactions) and in the design and synthesis of new organic sensitizers for unconventional photovoltaic cells production and photocatalysis.

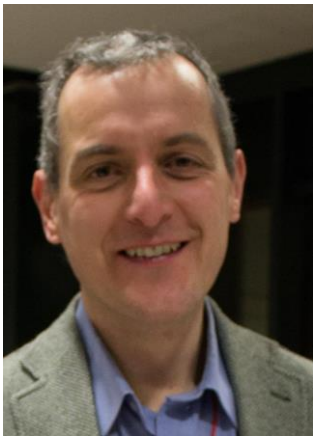

Lorenzo Zani was born in Florence, Italy. He studied chemistry at the University of Florence and in 2006 he completed his doctoral studies in organic chemistry at RWTH Aachen University, Germany, under the supervision of Prof. Carsten Bolm. He held postdoctoral positions at Stockholm University, Sweden, The Institute of Cancer Research, London, United Kingdom, and CNR-ICCOM, Sesto Fiorentino, Italy. Since 2011 he has been a CNR Researcher. His current research interests are in the fields of synthetic methodology and catalytic reactions, with a particular focus on preparation of new organic materials for energy conversion and photocatalytic hydrogen production.

Massimo Calamante studied Chemistry at the University of Pisa, where he graduated in 2002. He received his Ph.D. in Structural Biology at the University of Florence in 2007. After experiences in some private organic synthesis laboratories, in 2012 he started a post-doc collaboration with CNR-ICCOM (Sesto Fiorentino, Italy) and from 2013 he is a Researcher in the same institute. His research interests focus in the synthesis of organic molecues for photovoltaic application (DSSC, LSC) and photocatalytic hydrogen production.

Alessandro Mordini was born in Florence, Italy. He graduated in chemistry at the University of Florence in 1983 (supervisor Prof. Alfredo Ricci) and obtained his PhD degree at the same University in 1987 with the same supervisor. He held postdoctoral positions at Lausanne University, Switzerland (supervisor Prof. Manfred Schlosser) in 1986, 1989, and 1992. In 1987 he was appointed Researcher at CNR in Florence where he became Senior Researcher in 1999 and Director of Research in 2010 at the Institute of Organometallic Compounds (CNR-ICCOM) Sesto Fiorentino (FI), Italy. His research interest is in synthetic organic chemistry, especially in the field of carbanionic species (polar organometallics, metal-mediated rearrangements). More recent activities focus on the design and synthesis of new organic materials for energy production.

Alessio Dessì was born in Pescia (Italy) in 1987. He graduated in organic chemistry at the University of Pisa in 2012, then he received his PhD degree at the University of Florence in 2016, under the supervision of Dr. Gianna Reginato. After postdoctoral work at the Institute of Chemistry of OrganoMetallic Compounds (CNR-ICCOM) in Sesto Fiorentino (Italy), he is currently a researcher in the same institute. His main research activity regards the development of innovative and sustainable synthetic protocols for the preparation of photoactive organic materials and their application in the fields of photovoltaics and photocatalysis.